Molecular Therapy
Oncology
Original Article

Targeting CD45 by gene-edited CAR T cells for leukemia eradication and hematopoietic stem cell transplantation preconditioning

Valeria M. Stepanova,[1,2,8] Dmitry V. Volkov,[2,8] Daria S. Osipova,[1] Wenjian Wang,[3] Yingqin Hou,[3] Dmitry E. Pershin,[1] Mariia S. Fadeeva,[1] Ekaterina A. Malakhova,[1] Elena A. Kulakovskaya,[1] Lui Cuicui,[4] Zhao Mingfeng,[4] Hongkai Zhang,[5] Jia Xie,[6] Ding Zhang,[7] Ilgar Z. Mamedov,[1] Alexandr S. Chernov,[2] Georgij B. Telegin,[2] Yuri P. Rubtsov,[2] Alexander G. Gabibov,[2] Peng Wu,[3] Michael A. Maschan,[1] and Alexey V. Stepanov[7]

[1]Dmitry Rogachev National Medical Research Center of Pediatric Hematology, Oncology and Immunology, Moscow 117997, Russian Federation; [2]Shemyakin-Ovchinnikov Institute of Bioorganic Chemistry, Russian Academy of Sciences, Moscow 117997, Russian Federation; [3]Department of Molecular & Cellular Biology, The Scripps Research Institute, La Jolla, CA 92037, USA; [4]Department of Hematology, Tianjin First Central Hospital and College of Life Science, Tianjin 300384, China; [5]State Key Laboratory of Medicinal Chemical Biology and College of Life Sciences, Nankai University, 94 Weijin Road, Tianjin 300071, China; [6]Department of Chemistry, The Scripps Research Institute, La Jolla, CA 92037, USA; [7]Department of Integrative Structural and Computational Biology, The Scripps Research Institute, La Jolla, CA 92037, USA

Hematopoietic stem cell transplantation (HSCT) is widely used to treat patients with life-threatening hematologic and immune system disorders. Current nontargeted chemo-/radiotherapy conditioning regimens cause tissue injury and induce an array of immediate and delayed adverse effects, limiting the application of this life-saving treatment. The growing demand to replace canonical conditioning regimens has led to the development of alternative approaches, such as antibody-drug conjugates, naked antibodies, and CAR T cells. Here, we introduce a preconditioning strategy targeting CD45 on hematopoietic cells with CAR45 T cells. To avoid fratricide of CD45 CAR T cells, genomic disruption of the CD45 gene was performed on human CD45 CAR T cells in combination with the signaling kinase inhibitor dasatinib. CD45$^{\Delta}$ CAR45 T cells showed high cytotoxicity *in vitro* and depletion of tumor cells *in vivo*. These cells were effective in elimination of human hematopoietic cells engrafted in humanized immunodeficient mice by transfusion with human blood-derived hematopoietic stem cells (HSCs). Similarly, CD45$^{\Delta}$ CAR45 natural killer (NK) cells exhibited potent cytotoxicity toward tumor cell lines and human hematopoietic cells *in vitro*. Thus, we provide the proof of concept for the generation and preclinical efficacy of fratricide-resistant CAR45 T and NK cells directed against CD45-expressing tumors and hematopoietic cells.

INTRODUCTION

To achieve the successful engraftment of allogeneic hematopoietic stem cells (HSCs) for HSC transplantation (HSCT), patients undergo chemotherapy and/or radiotherapy at doses that are highly toxic to blood and bone marrow cells. Approved pretreatment regimens are well tolerated by nonhematopoietic tissues (in most patients). However, multiorgan toxicity associated with conditioning is a limiting factor for safe and widespread allogeneic HSCT.[1,2] Patients with genetic disorders such as Fanconi anemia and Nijmegen syndrome have poor tolerance to standard genotoxic preparative regimens due to hypersensitivity to DNA damage.[3–5] This makes HSCT risky for these patients and results in an exceedingly low success rate for patients with secondary leukemias arising from underlying DNA repair lesions.

There is a considerable interest in replacing chemotherapy or radiotherapy with nongenotoxic preparative regimens. A variety of agents, such as antibody radioconjugates,[6–9] antibody-drug conjugates,[10–13] and naked antibodies,[14–17] have been developed to effectively deplete hematopoietic lineages *in vivo* to enable alloengraftment. However, the eradication of highly aggressive and treatment-resistant malignant hematopoietic cells may require less toxic and more potent cell-based therapies. Preclinical studies have shown that myeloablation using chimeric antigen receptor (CAR) T cells specific for CD117,[18,19] CD33,[20] and CD123[21,22] can successfully eliminate HSCs and hematopoietic progenitor cells. These antigens are rational targets for CAR T cells because they are expressed on HSCs or

Received 7 November 2023; accepted 25 June 2024;
https://doi.org/10.1016/j.omton.2024.200843.

[8]These authors contributed equally

Correspondence: Peng Wu, The Scripps Research Institute, 10550 N. Torrey Pines Road, La Jolla, CA 92037, USA.
E-mail: pengwu@scripps.edu
Correspondence: Michael A. Maschan, Dmitry Rogachev National Medical Research Center of Pediatric Hematology, Oncology and Immunology, 1 Samory Mashela Street, Moscow 117997, Russia.
E-mail: michael.maschan@fccho-moscow.ru
Correspondence: Alexey V. Stepanov, The Scripps Research Institute, 10550 N. Torrey Pines Road, La Jolla, CA 92037, USA.
E-mail: stepanov@scripps.edu

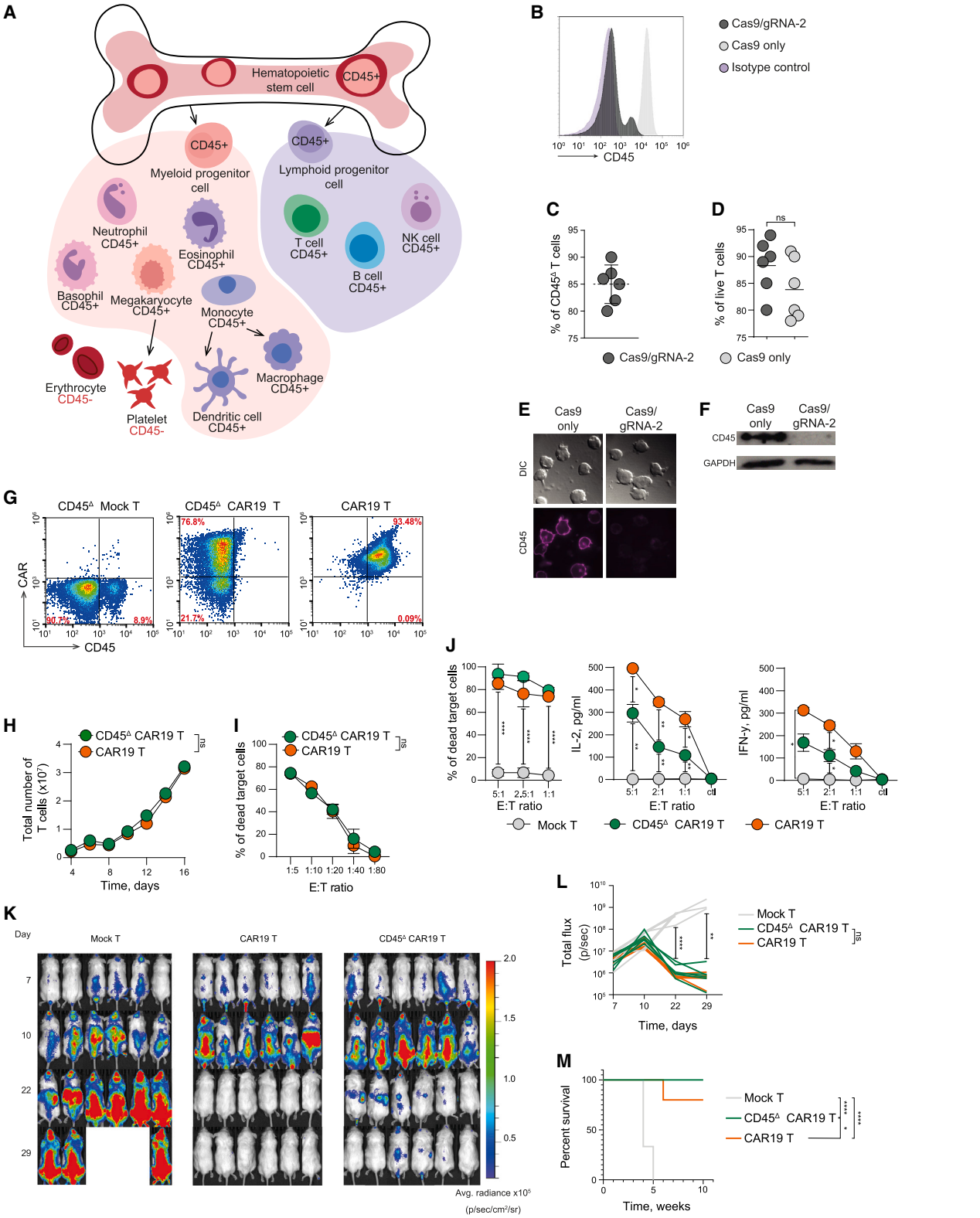

(legend on next page)

hematopoietic progenitor cells (HPCs) with minimal or no expression on nonhematopoietic tissues.

The receptor tyrosine phosphatase CD45 is a cell-surface antigen present on all immune and hematopoietic cells, including HSCs and HPCs, with the exception of platelets and erythrocytes,[23] which makes targeting CD45 particularly suitable for a conditioning regimen prior to HSCT. CD45 expression patterns in the bone marrow of patients with various types of acute leukemia clearly show the prevalence of CD45-positive cells.[24–27] In recent decades, CD45 has been one of the most attractive targets for nonmyeloablative regimens using antibodies, immunotoxins, and antibody-drug conjugates (ADCs).[6–8,12,13,16,28–30]

In contrast to CD117, CD33, and CD123, CD45 is one of the most abundant proteins in the T cell plasma membrane. Shared target-antigen expression between CAR T cells and target cells is a major challenge that complicates CAR T cell therapies. Since the development of CD5-specific gene-edited T cells, fratricide-resistant CAR T cells have become a rapidly growing class of leukemia immunotherapy.[31] Recent studies have demonstrated the feasibility of fratricide-resistant CARs targeting CD3,[32] CD5[31,33] and CD7[34–38] (CD5/CD7 bispecific[35]), and CD38.[39,40] Some of these approaches are being tested in early phase clinical trials, with encouraging results (NCT04004637, ChiCTR2000034762, and NCT03690011; clinicaltrials.gov).

Here, we describe the generation of CAR T cells directed against human CD45 as a proof of concept for leukemia therapy and nongenotoxic conditioning prior to HSCT. A regimen bridging HSCT preconditioning and leukemia therapy using leukocyte-specific CAR T cells may allow for more comprehensive depletion of the hematopoietic cells with a minimized risk of residual disease or relapse after transplantation. To improve the translational potential of this approach, the CAR45 construct was designed to consist of the anti-CD45 antibody BC8, which has been extensively tested in clinical trials (NCT00002554, NCT00003868, NCT00003870, NCT00005940, NCT00008177, NCT00988715, NCT01300572, NCT01503242, and NCT01921387; clinicaltrials.gov), fused with the third-generation CAR backbone.

To overcome CD45-dependent fratricide during the CAR45 T cell manufacturing process and after infusion, we performed targeted disruption of the CD45 gene using CRISPR-Cas9. We showed that gene editing and CAR transduction protocols consistently yield a highly enriched population of CD45-negative CAR45 T and natural killer (NK) cells (CD45$^{\Delta}$ CAR45). The CD45$^{\Delta}$ CAR45 T cells demonstrate robust antitumor activity against hematological malignancies and normal human hematopoietic cells *in vitro* and *in vivo*. If successful, fratricide-resistant CD45$^{\Delta}$ CAR45 T cells could serve as an alternative nongenotoxic tool to eradicate both normal and pathologic hematopoietic cells, ensuring engraftment and clearance of the leukemia burden while sparing nonhematopoietic tissue, mature platelets, and red blood cells.

RESULTS

PTPRC gene editing in human T cells for pan-hematologic cancer immunotherapy

The expression patterns of CD45 in the bone marrow of patients with various types of acute leukemia make it a promising target in the context of hematological malignancies. Targeting CD45 could serve a dual purpose as a conditioning regimen prior to HSCT and as a pan-hematologic cancer immunotherapy (Figure 1A). CRISPR-Cas9-mediated genome editing was implemented to disrupt the *PTPRC* gene (encoding the CD45 protein) in T cells to prevent fratricide during the production and expansion of CD45-specific CAR T (CAR45) cells (Figure 2A). Different guide RNAs (gRNAs) targeting exon 1 of the *PTPRC* gene were designed to prevent translation of all possible isoforms of CD45. gRNAs were tested in activated human T cells, and gRNA-2 (Figure S1A), which disrupted the *PTPRC* gene with the highest efficiency, was chosen for future experiments. Loss of surface CD45 expression was observed in >85% of T cells 4 days after electroporation with gRNA-2 and Cas9, compared to Cas9 alone (Figures 1B, 1C, and S1B). The knockout of CD45 did not result in significant changes in T cell viability (Figure 1D), and CD45 ablation was stable for at least 4 weeks (Figure S1C). Loss of CD45 expression was further confirmed by confocal microscopy and western blot analysis of the fluorescence-activated cell sorting (FACS)-sorted cells with disrupted *PTPRC* gene (Figures 1E, 1F, and S1D). Analysis of the targeted fragment in PCR-amplified

Figure 1. Disruption of CD45 expression does not impair the functional activity of T cells and CAR T cells

(A) CD45 expression on different cells during hematopoiesis. (B) Representative histogram showing ablation of CD45 expression in T cells after electroporation with CRISPR-Cas9 and CD45-specific gRNA-2. (C and D) Frequency and viability of CD45-negative cells on the fourth day after electroporation with Cas9/gRNA-2 complexes. The *p* values were determined by multiple unpaired t tests. Each dot represents an independent donor. (E) Fluorescence microscopy of T and CD45$^{\Delta}$ T cells stained with anti-CD45 antibodies (magenta) after FACS. (F) Western blot analysis of CD45 expression in T cells from (B) after FACS. (G) Representative dot plots showing the expression of CAR19 and CD45 in mock-transduced, CAR19, and CD45$^{\Delta}$ CAR19 T cells. (H) Total expansion of CAR19 and CD45$^{\Delta}$ CAR19 T cells after 14 days of *in vitro* culture. The *p* values were determined by multiple unpaired t tests. (I) Nalm-6 cells were incubated with different numbers of CAR19 and CD45$^{\Delta}$ CAR19 T cells prior to analysis of tumor cell lysis. The *p* values were determined by multiple unpaired t tests. (J) IL-2 and IFN-γ secretion and target cell killing by mock-transduced, CAR19, and CD45$^{\Delta}$ CAR19 T cells mixed with Jeko-1 cells at different effector (E)-to-target (T) ratios. The *p* values were determined by multiple unpaired t tests. Nonsignificant values are not shown. (K) Representative IVIS images of mice from the mock-transduced, CAR19, and CD45$^{\Delta}$ CAR19 T cell-treated groups. NCG mice were implanted i.v. with 1×10^6 Nalm-6/ffluc cells. On day 7 after tumor inoculation, the animals were subjected to i.v. infusion of 3×10^6 mock-transduced, CAR19, or CD45$^{\Delta}$ CAR19 T cells ($n = 6$). (L) Quantification of tumor burden (as the total radiance due to luciferase activity per mouse) from (K) for days 7–29. The *p* values were determined by multiple unpaired t tests. (M) Survival plots for animals from the experimental and control groups. Overall survival curves were plotted using the Kaplan-Meier method and compared using the log-rank (Mantel-Cox) test. Data from (B) and (E)–(J) represent independent replicated experiments with cells isolated from three donors. All data represent the mean ± SD. ns indicates $p > 0.05$, * indicates $p \leq 0.05$, ** indicates $p \leq 0.01$, **** indicates $p \leq 0.0001$.

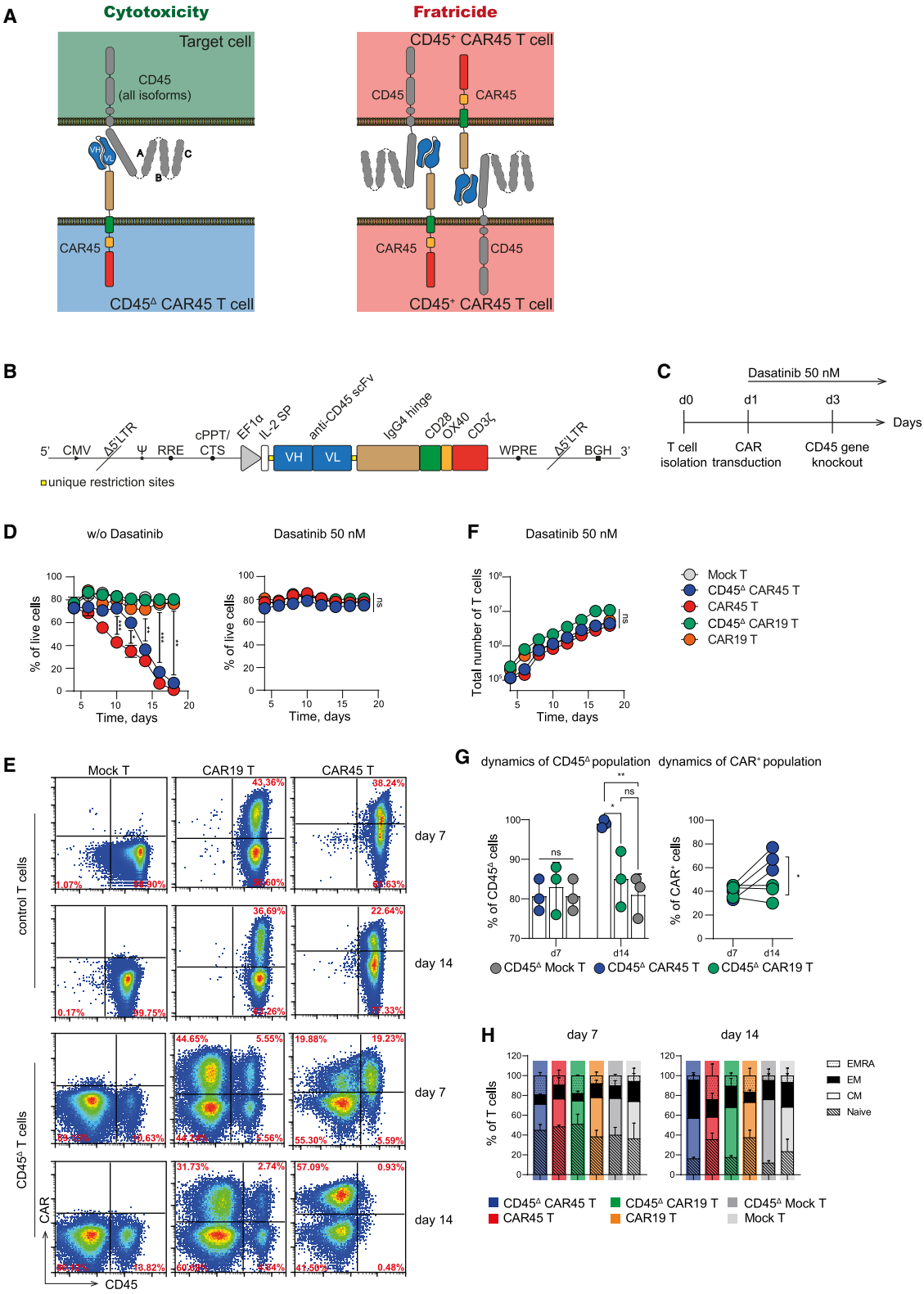

(legend on next page)

genomic DNA by Sanger sequencing revealed the presence of insertions/deletions (indels) in the CD45 gene only in the CD45$^{\Delta}$ T cells (Figure S1E). Potential off-target sites for gRNA-2 were verified by next-generation sequencing of gene-edited T cell genomic DNA. The percentage of reads containing insertions and deletions increased from 70% to 90% with the increase in knockout percentage over time exclusively in CD45$^{\Delta}$ T cells (4, 8, and 16 h following electroporation with Cas9/gRNA-2) (Figure S1F). For gRNA-2, only one off-target site with the highest predicted probability had a higher percentage of both insertions and deletions in cells treated with the Cas9/gRNA-2 complex compared to a negative control (0.5%; $p < 0.001$). It is located in the intron of the *THSD4* gene, which is transcriptionally silent in the immune cells (Table S1). These results suggest that Cas9/gRNA-2-mediated disruption of exon 1 in the *PTPRC* gene effectively generates viable CD45$^{\Delta}$ T cells.

Genetic disruption of the CD45 gene does not impair T or CAR T cell functions

We then asked whether disruption of *PTPRC* and absence of the CD45 cytoplasmic domain as well as the associated phosphatase activity affect T cell function. First, we compared the cytotoxicity and cytokine release of T and CD45$^{\Delta}$ T cells by incubation with Burkitt lymphoma Ramos cells in the presence of a bispecific CD19/CD3 T cell engager (BiTE) (Figure S2A). Interestingly, T and CD45$^{\Delta}$ T cells exhibited comparable cytotoxic activity with relatively less interleukin-2 (IL-2) and interferon-γ (IFN-γ) secreted by CD45$^{\Delta}$ T cells (Figures S2B and S2C). These results suggest that genetic knockout of CD45 in T cells does not affect their cytotoxic potential but slightly downmodulates the secretion of proinflammatory cytokines.

The high cytolytic activity of CD45$^{\Delta}$ T cells encouraged us to further evaluate the effect of *PTPRC* gene disruption on CAR T cell performance. First, T cells were electroporated with CRISPR-Cas9 and CD45-specific gRNA-2 or control gRNA and then transduced with CD19-specific CAR19 (Figure 1G). In comparison to CAR19 T cells, the loss of CD45 did not reduce the proliferation rate of CD45$^{\Delta}$ CAR19 T cells when stimulated under the same conditions (Figure 1H). CAR19 and CD45$^{\Delta}$ CAR19 T cells were then co-cultured with target CD19^{+} Nalm-6 and Jeko-1 cells. Both CAR19 and CD45$^{\Delta}$ CAR19 T cells efficiently induced the lysis of target tumor cells after 24 h of co-culturing (Figures 1I and 1J, left). Consistent with what we observed in the BiTE-mediated T cell activation experiment, compared to CAR19 T cells, CD45$^{\Delta}$ CAR19 T cells secreted slightly less IL-2 and IFN-γ when incubated with target cells (Figure 1J, middle and right).

Then, we explored the cytotoxic function of CD45$^{\Delta}$ CAR19 T cells *in vivo* in a mouse xenograft model of pre-B cell lymphoma Nalm-6. NOD-severe combined immunodeficiency (SCID) γ-chain-deficient (NCG) mice were intravenously (i.v.) engrafted with Nalm-6/ffluc cells expressing firefly luciferase (ffluc). On day 7 following Nalm-6 injection, when the tumors became detectable, the mice were i.v. injected with a single dose of 2×10^6 CD45$^{\Delta}$ CAR19, CAR19, or mock-transduced T cells. Bioluminescence *in vivo* imaging revealed a significant tumor burden reduction in the CAR19 and CD45$^{\Delta}$ CAR19 therapy groups (Figure 1K). And no apparent differences in tumor growth kinetics were observed between the groups of mice treated with regular or CD45$^{\Delta}$ CAR19 T cells (Figure 1L). A slightly higher survival rate of recipient mice following injections of CD45$^{\Delta}$ CAR19 T cells was observed compared to mice treated with regular CAR19 T cells (Figure 1M). Therefore, CD45 knockout had no negative effect on the short-term persistence or cytotoxicity of CAR T cells in the mouse tumor xenograft model.

Generation of fratricide-resistant CD45-specific CAR T cells

After obtaining experimental proof that CD45$^{\Delta}$ CAR19 T cells possess potent antitumor activity and persistence in mice, we next explored whether CD45 knockout allows generation of fratricide-resistant CAR T cells specific to CD45 (Figure 2A). We created a CAR45 construct by fusing a single-chain variable fragment derived from the murine anti-CD45 monoclonal antibody (clone BC8) to a third-generation CAR backbone containing the IgG4 CH2-CH3 spacer and cytoplasmic endodomains from CD28, CD134, and CD3ζ[41,42] (Figure 2B). CD45 knockout was performed 2 days after T cell transduction with the CAR45 and CAR19 constructs (Figure 2C). However, in contrast to the control CAR19 and CD45$^{\Delta}$ CAR19 T cells, both CD45$^{\Delta}$ CAR45 and CAR45 T cells showed poor viability and expansion, presumably due to antigen-induced fratricide and chronic stimulation in response to residual amounts of CD45 left on T cells (Figure 2D, left). This result was later verified on days 7 and 14 post knockout (Figure 2E). Previous studies have shown that treatment with dasatinib[43] inhibits cytolytic activity, cytokine production, and proliferation of CAR T cells *in vitro* and *in vivo*. Inspired by these pioneering studies, we assessed whether dasatinib treatment can suppress the fratricide and enhance the survival of CD45-specific CAR T cells (Figure S3). The CAR T cell production

Figure 2. Generation of fratricide-resistant CD45-specific CAR T cells

(A) Experimental setup for CD45$^{\Delta}$ CAR T cell engineering. T cells were electroporated with Cas9/gRNA-2 complexes and transduced with CAR. (B) Schematic of CAR45 construct design. (C) Schematic timeline of CD45$^{\Delta}$ CAR T cell engineering. (D) Effects of 50 nM dasatinib on the viability of CAR19, CAR45, CD45$^{\Delta}$ CAR19, and CD45$^{\Delta}$ CAR45 T cells in culture. The *p* values were determined by multiple unpaired t tests. (E) Representative dot plots showing the expression of CD45 and CARs in control and Cas9/gRNA-2-electroporated T cells on days 7 and 14 after transduction. (F) Total expansion of cells from (D), right. The *p* values were determined by multiple unpaired t tests. (G) Percentage of CD45$^{\Delta}$ CAR T cells in (E). The *p* values were determined by multiple unpaired t tests. (H) Differentiation state analysis of CAR19-, CAR45-, and mock-transduced T cells electroporated with Cas9/gRNA-2. Cells were stained with anti-CD44 and anti-CD62L antibodies and analyzed by flow cytometry on days 7 and 14 after transduction. CM, central memory; EM, effector memory; EMRA, terminally differentiated T cells. The *p* values were determined by two-way ANOVA. Data from (D)–(H) represent independent experiments with cells isolated from five donors. All data represent the mean ± SD. ns indicates $p > 0.05$, * indicates $p \leq 0.05$, ** indicates $p \leq 0.01$, *** indicates $p \leq 0.001$.

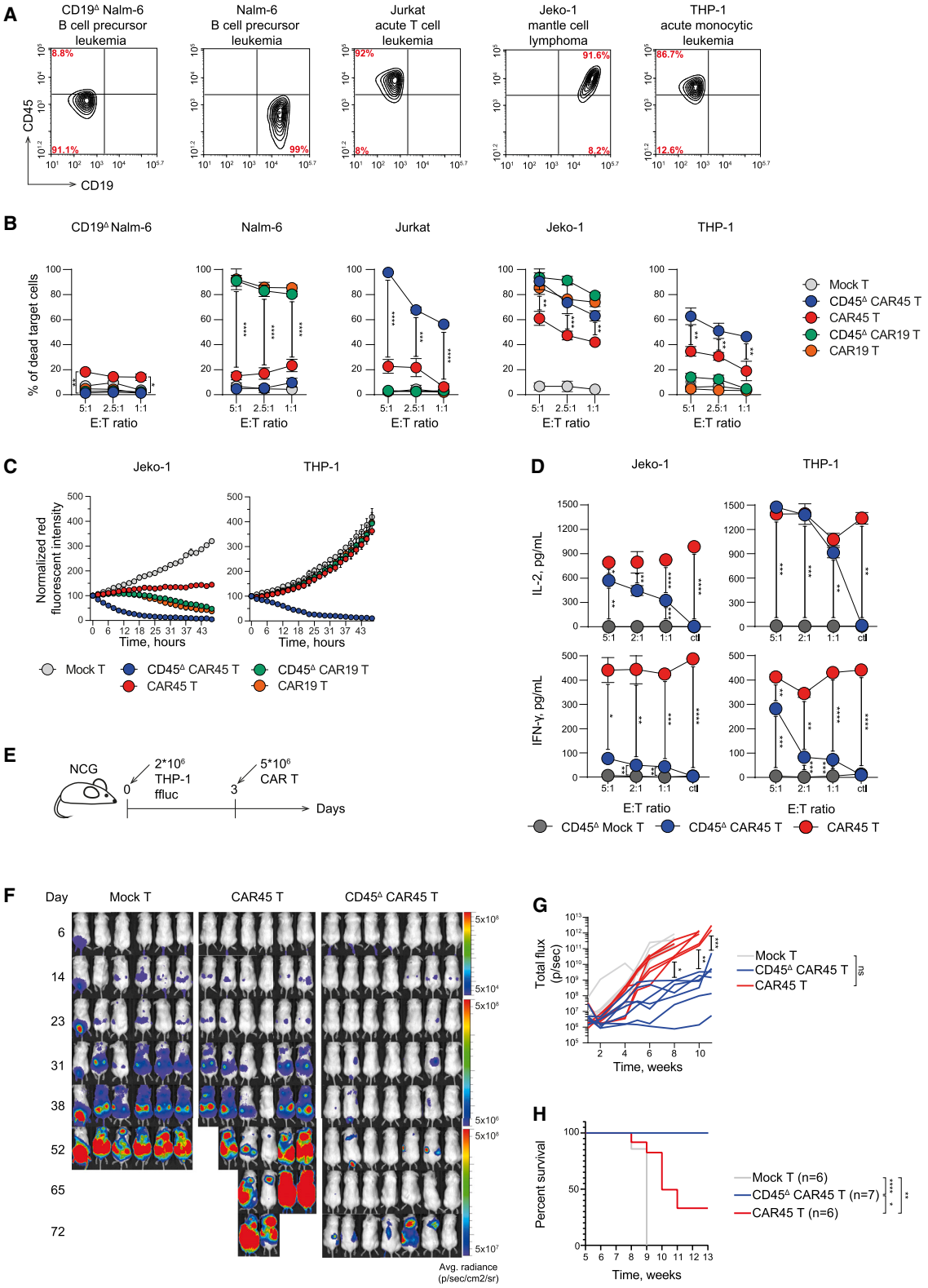

(legend on next page)

was then repeated with addition of dasatinib to the culture medium right after transduction. To maintain the effective concentration, the medium was replenished with fresh dasatinib every 2–3 days. By dosing the concentration, we found that dasatinib rescued the expansion and viability of both CAR45 and CD45$^{\Delta}$ CAR45 T cells at concentrations of 50 nM or higher (Figures 2D, right, and 2F). Interestingly, in the culture of CD45$^{\Delta}$ CAR45 T cells, despite the administration of dasatinib, we observed the elimination of residual CD45-positive cells and the outgrowth of the CD45$^{\Delta}$ CAR45 population on day 14 (Figure 2G). CD45 knockout did not negatively alter the T cell phenotype, but instead produced T cells with predominantly central memory (Tcm) and effector memory (Tem) phenotypes, a favorable property for tumor control (Figure 2H).

CD45$^{\Delta}$ CAR45 T cells outperform CAR45 T cells *in vitro* and *in vivo*

To assess whether CD45$^{\Delta}$ CAR45 T cells maintained their functionality, we analyzed the specificity and cytotoxicity of CD45$^{\Delta}$ CAR45 T cells against CD45-positive T-ALL (Jurkat), MCL (Jeko-1), and AML (THP-1) cells and a CD45-negative (Nalm-6) tumor cell line (Figure 3A). The fresh batches of CAR19, CAR45, CD45$^{\Delta}$ CAR19, and CD45$^{\Delta}$ CAR45 T cells were produced from the same donor and expanded with 50 nM dasatinib. After removal of dasatinib, CAR T cells were co-cultured with a panel of hematological tumor cell lines with varying expression of CD19 and CD45 (Figure 3A). As expected, CAR19 and CD45$^{\Delta}$ CAR19 T cells induced the specific killing of CD19-positive Nalm-6 and Jeko-1 cells with similar efficacies (Figure 3B) and kinetics (Figure 3C). CAR19 and CD45$^{\Delta}$ CAR19 T cells were not cytotoxic to control CD19-knockout Nalm-6 cells (Figure 3C). However, we observed a significant difference in cytotoxicity and cytokine release between CAR45 and CD45$^{\Delta}$ CAR45 T cells. In comparison to CAR45 T cells, CD45$^{\Delta}$ CAR45 T cells induced pronouncedly more effective killing of CD45-positive Jurkat, Jeko-1, and THP-1 cells (Figure 3B). At a low effector:target (E:T) ratio (1:3), the CD45$^{\Delta}$ CAR45 T cells eliminated tumor cells faster than CAR45 T cells (Figure 3C). In addition, we discovered that CAR45 T cells exhibited nonspecific hyperactivation, accompanied by elevated production of IL-2 and IFN-γ, which was independent of the E:T ratio, even in the absence of target cells. By contrast, CD45$^{\Delta}$ CAR45 T cells released cytokines only upon incubation with target cells in a manner dependent on the E:T ratio (Figure 3D).

Following these *in vitro* tests, we analyzed the therapeutic efficacy of CD45$^{\Delta}$ CAR45 T cells in a mouse xenograft model of disseminated monocytic AML. Toward this end, NCG mice were engrafted via i.v. injection of 2×10^6 THP-1/ffluc cells expressing ffluc (Figure 3E). Three days after tumor engraftment, the animals were i.v. injected with 5×10^6 mock, CAR45, or CD45$^{\Delta}$ CAR45 T cells. Bioluminescence imaging revealed the outstanding therapeutic activity of CD45$^{\Delta}$ CAR45 T cells against disseminated monocytic AML (Figure 3F). All animals treated with CD45$^{\Delta}$ CAR45 T cells exhibited significant suppression of tumor burden and higher survival rates compared to the counterparts treated with mock or CAR45 (Figures 3G, 3H, and S4).

CD45$^{\Delta}$ CAR45 T and NK cells deplete human hematopoietic cells *in vitro*

Our ultimate goal is to determine whether CD45$^{\Delta}$ CAR45 T cells can be used to deplete endogenous hematopoietic cells. Toward this end, we incubated primary human T cells and peripheral blood mononuclear cells (PBMCs) with CD45$^{\Delta}$ CAR45 T cells or control CD45$^{\Delta}$ CAR19 T. After 24 h of co-culture, CD45$^{\Delta}$ CAR45 T cells, but not control CD45$^{\Delta}$ CAR19 T cells, induced productive killing of T cells and PBMCs (Figure 4A). To assess the kinetics of hematopoietic cell depletion, we mixed PBMCs and FACS-purified CD45-negative CD45$^{\Delta}$ CAR45 T cells in a 1:3 ratio and followed the changes in their ratio for over 72 h (Figure 4B). A negative control group was supplemented with 50 nM dasatinib. We observed complete elimination of PBMCs in the experimental group after 72 h of co-culture, while the PBMCs in the control group remained viable (Figure S5A). We also performed a dose-dependent test with different concentrations of dasatinib and found that concentrations below 50 nM turned on CD45-dependent killing (Figure S5B). Likewise, CD45$^{\Delta}$ CAR45 T cells also induced efficient killing of freshly isolated autologous donor bone marrow (BM) cells, and the killing could be inhibited by 50 nM dasatinib (Figure S6).

CAR NK cells are attractive substitutes for traditional CAR T cells owing to their potent cytotoxicity and diminished risk of alloreactivity.[44] Another advantage of CAR NK cells is their shorter lifespan compared to CAR T cells, which makes them suitable for transient immunotherapy.[45] Therefore, the feasibility of generating functional fratricide-resistant CD45$^{\Delta}$ CAR45 NK cells was tested. The protocol

Figure 3. CD45$^{\Delta}$ CAR45 T cells outperform CAR45 T cells *in vitro* and *in vivo*

(A) Representative density plots showing the expression of CD19 and CD45 in leukemia and lymphoma cell lines. (B) CAR19, CAR45, CD45$^{\Delta}$ CAR19, and CD45$^{\Delta}$ CAR45 T cells were incubated with blood cancer cell lines prior to tumor cell lysis analysis. Total numbers of live tumor cells were quantified by flow cytometry at 24 h using counting beads. The *p* values were determined by multiple unpaired t tests. Nonsignificant values are not shown. (C) Real-time detection of fluorescent Jeko-1 and THP-1 targets incubated with the designated CAR19, CAR45, CD45$^{\Delta}$ CAR19, and CD45$^{\Delta}$ CAR45 T cells in the Incucyte killing assay (E:T ratio 1:3). (D) Quantification of IFN-γ and IL-2 secretion by CAR45 and CD45$^{\Delta}$ CAR45 T cells co-cultured with Jeko-1 and THP-1 cells. The *p* values were determined by multiple unpaired t tests. (E) NCG mice were subjected to i.v. infusion of 2×10^6 THP-1/ffluc cells. On day 3 after tumor inoculation, animals were subjected to i.v. infusion of 3×10^6 mock-transduced, CAR45, or CD45$^{\Delta}$ CAR45 T cells. (F) Representative IVIS images of mice from the mock-transduced, CAR45, and CD45$^{\Delta}$ CAR45 T cell-treated groups. (G) Quantification of tumor burden (as the total radiance due to luciferase activity per mouse) from (F) for days 7–29. The *p* values were determined by multiple unpaired t tests. (H) Kaplan-Meier curve showing overall animal survival in each experimental group. The *p* values were determined by the log-rank Mantel-Cox test. Data from (B)–(D) represent independent experiments with cells isolated from three donors (biological replicates). All data represent the mean ± SD. ns indicates $p > 0.05$, * indicates $p \leq 0.05$, ** indicates $p \leq 0.01$, *** indicates $p \leq 0.001$, **** indicates $p \leq 0.0001$.

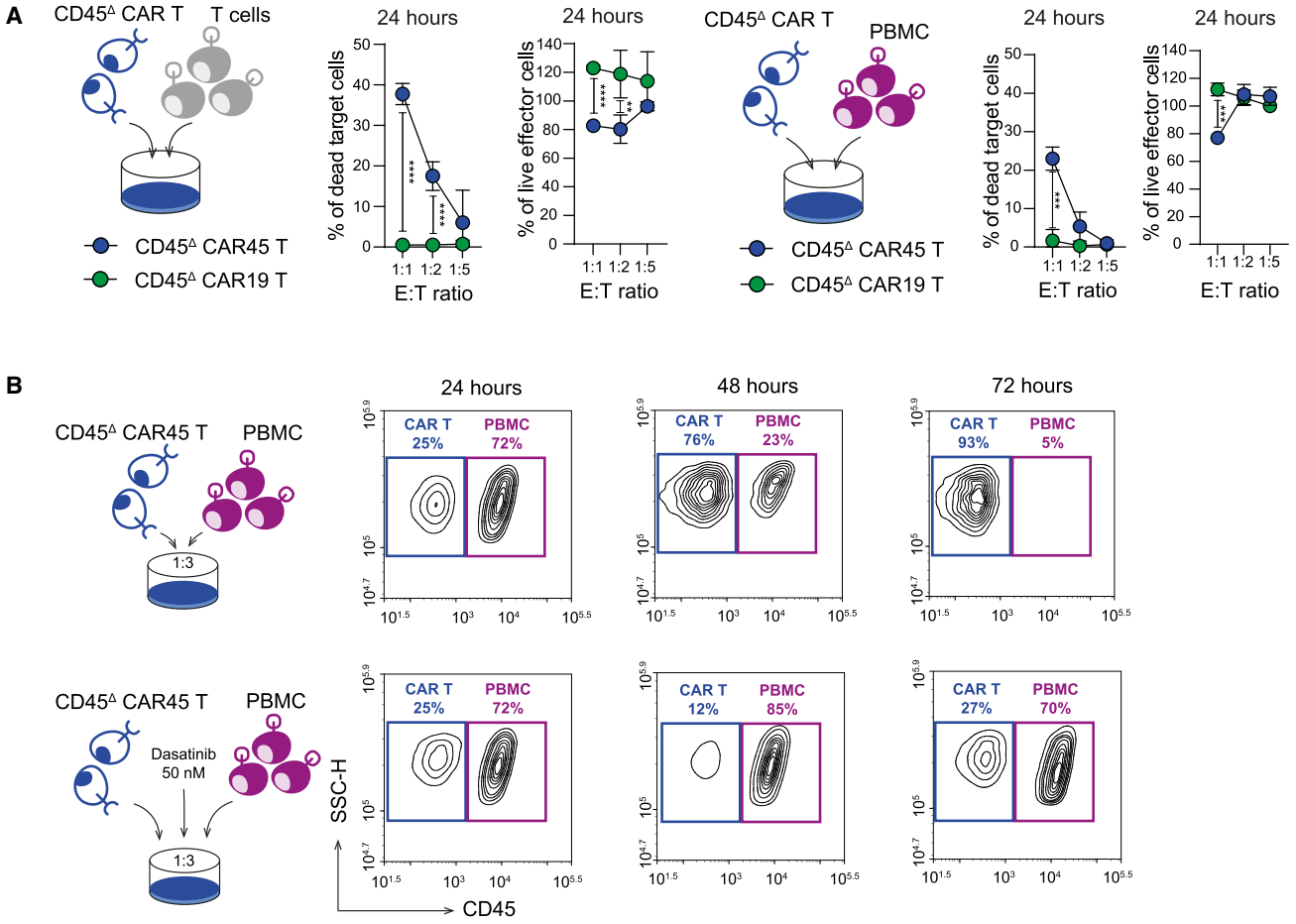

Figure 4. Cytotoxicity and specificity of CD45$^{\Delta}$ CAR45 T cells against primary human cells

(A) Freshly isolated human T cells or PBMCs were co-cultured with CD45$^{\Delta}$ CAR19 and CD45$^{\Delta}$ CAR45 T cells. Total numbers of live target cells were quantified by flow cytometry at 24 h using counting beads. The percentage of cell counts was normalized to the starting cell number. The *p* values were determined by multiple unpaired t tests. Nonsignificant values are not shown. (B) Freshly isolated PBMCs were co-cultured with CD45$^{\Delta}$ CAR45 T cells at a 1:3 ratio for 24, 48, and 72 h upon addition of 50 nM dasatinib or no drug. Contour plots show the frequency of live PBMCs at the end of the co-culture period. Data represent independent experiments with cells isolated from three donors. ** indicates $p \leq 0.01$, *** indicates $p \leq 0.001$, **** indicates $p \leq 0.0001$.

used for *PTPRC* gene disruption and CAR transduction was optimized for human NK cells (Figure 5A). CD45 knockout was highly effective and did not alter NK cell viability or proliferation, and the CAR45 transduction efficacy was greater than 50% (Figure 5B). CD45$^{\Delta}$ CAR45 NK cells were expanded in cultures supplemented with 50 nM dasatinib to avoid undesired fratricidal effects. Compared to CAR45 NK, CD45$^{\Delta}$ CAR45 NK cells demonstrated a superior ability to induce the killing of autologous T cells and PBMCs following 4 and 24 h of incubation (Figure 5C). These results support the potential implementation of fratricide-resistant CD45$^{\Delta}$ CAR45 NK cells for adoptive immunotherapy.

Autologous CD45$^{\Delta}$ CAR45 T cells target and deplete hematopoietic cells in humanized hu-PBMC-NCG mice

We next determined whether conditioning with CD45$^{\Delta}$ CAR45 T cells enables successful depletion of engrafted donor hematopoietic cells in human PBMC-engrafted NCG mice (hu-PBMC-NCG), which were generated by transferring 20×10^6 PBMCs from a healthy donor into NCG mice (Figure 6A). Four weeks after PBMC engraftment, double staining of blood samples with antihuman and antimouse CD45 antibodies was performed to assess chimerism in the animals (Figure 6B). Successful engraftment occurred in all animals, with 40%–60% of the cells found to be of human origin 4 weeks after PBMC injection. The humanized mice were divided randomly into three groups ($n = 8$) and subjected to i.v. injection of 10×10^6 CD45$^{\Delta}$ CAR45, CD45$^{\Delta}$ CAR19, or CD45$^{\Delta}$ mock-transduced T cells from the same PBMC donor. Mice treated with CD45$^{\Delta}$ CAR45 T cells exhibited a decreasing number of engrafted human PBMCs 4 weeks after injection. A significant decrease in human PBMCs was observed at week 8 (Figures 6B and 6D). By contrast, animals injected with CD45$^{\Delta}$ CAR19 or CD45$^{\Delta}$ mock-transduced T cells maintained stable or even increasing levels of humanization. Analysis of

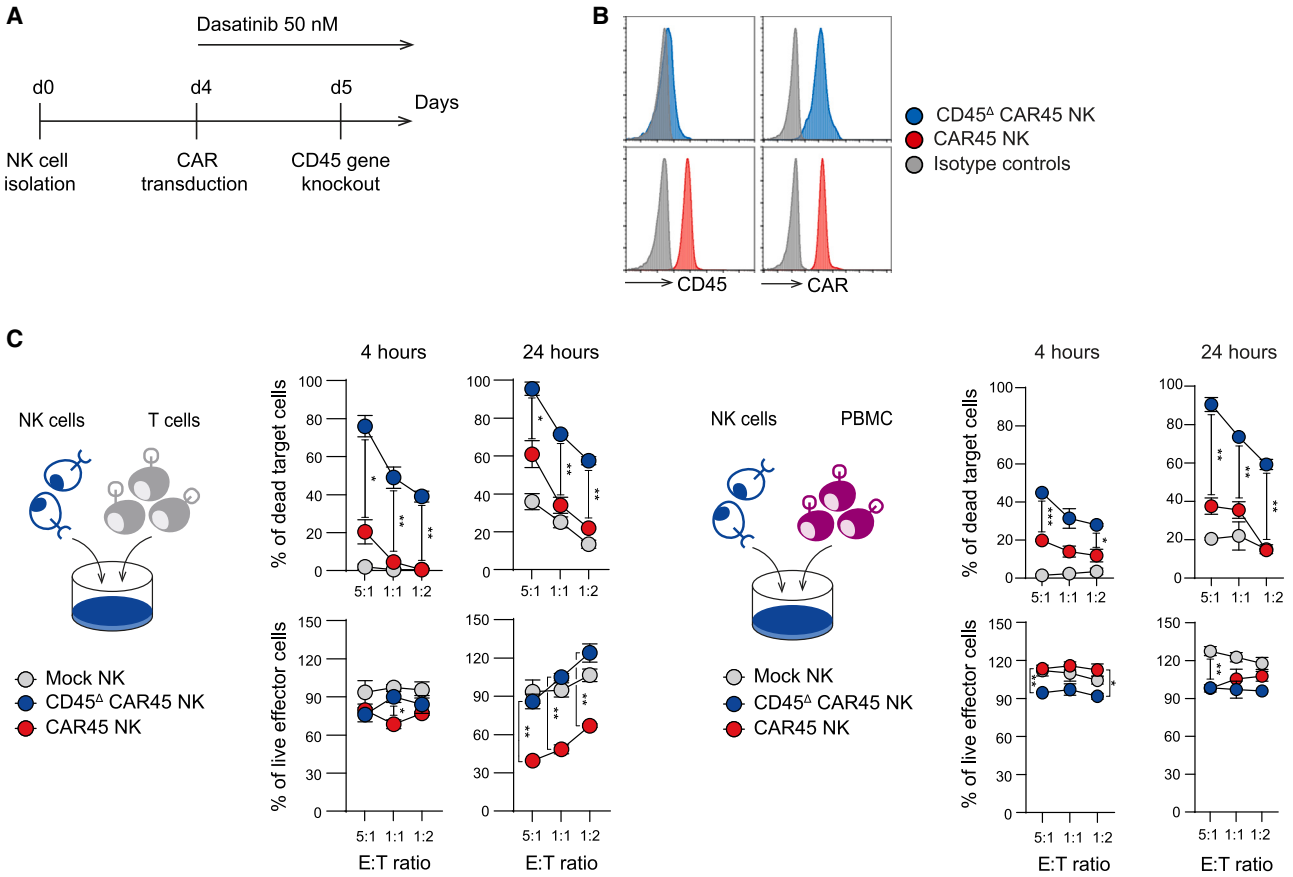

Figure 5. Cytotoxicity and specificity of CD45$^{\Delta}$ CAR45 NK cells against primary human cells

(A) Schematic of the CD45$^{\Delta}$ CAR NK cell engineering timeline. (B) Representative histograms showing the expression of CD45 and CAR45 in control and Cas9/gRNA-2-electroporated NK cells on day 14 after transduction. (C) Freshly isolated autologous human T cells or PBMCs were co-cultured with CAR45 and CD45$^{\Delta}$ CAR45 NK cells. Total numbers of live CAR and target cells were quantified by flow cytometry at 4 and 24 h. The percentage of cell counts was normalized to the starting cell number. The *p* values were determined by multiple unpaired t tests. Nonsignificant values are not shown. Data from (B) and(C) represent independent experiments with cells isolated from three donors (biological replicates). All data represent the mean ± SD. * indicates $p \leq 0.05$, ** indicates $p \leq 0.01$, *** indicates $p \leq 0.001$.

the persistence of human cells in the blood showed the consistent presence of only CD45$^{\Delta}$ CAR45 T cells, which accounted for approximately 25% of the total CD3^{+} T cells (Figures 6C and 6E). Typically, hu-PBMC-NCG mice develop a xenogeneic response resembling GvHD 4–5 weeks following human PBMC injection. This is consistent with the survival time of animals treated with CD45$^{\Delta}$ CAR19 or CD45$^{\Delta}$ mock-transduced T cells. However, the effective elimination of hPBMCs by CD45$^{\Delta}$ CAR45 T cells dramatically delayed the development of graft-versus-host disease (GvHD) -like symptoms and prolonged the survival of the humanized mice by 40 days (65 days vs. 105 days, respectively; $p = 0.0092$) (Figure 6F).

It is important to acknowledge the limitations of this hu-PBMC-NCG model that made it possible to evaluate the *in vivo* efficacy of CD45$^{\Delta}$ CAR45 T cells against healthy human primary cells. However, only studies using mice with an intact immune system that are conditioned with murine antimouse CD45 CAR T cells would allow the assessment of potential CAR T trafficking issues, which have been previously reported to be the reason for reduced efficacy of murine CD117-CAR T cells[18] but not human CD117-CAR T cells in NSG mice engrafted with AML patient BM.[19]

DISCUSSION

The consideration of using CAR T cells or antibody-drug conjugates for pre-HSCT conditioning stems from the clinically observed toxicity and side effects of ionizing radiation and potent alkylating agents such as busulfan. Such agents carry the risk of damaging or inflaming both the bone marrow and the thymic stroma, potentially hindering optimal bone marrow engraftment and eventual reconstitution of lymphoid immunity.[46]

Several antigens, including CD117, CD123, CD33, and others, have been considered as potential targets for HSCT conditioning via antibody- or CAR T-based agents. Data on an anti-CD117 antibody and

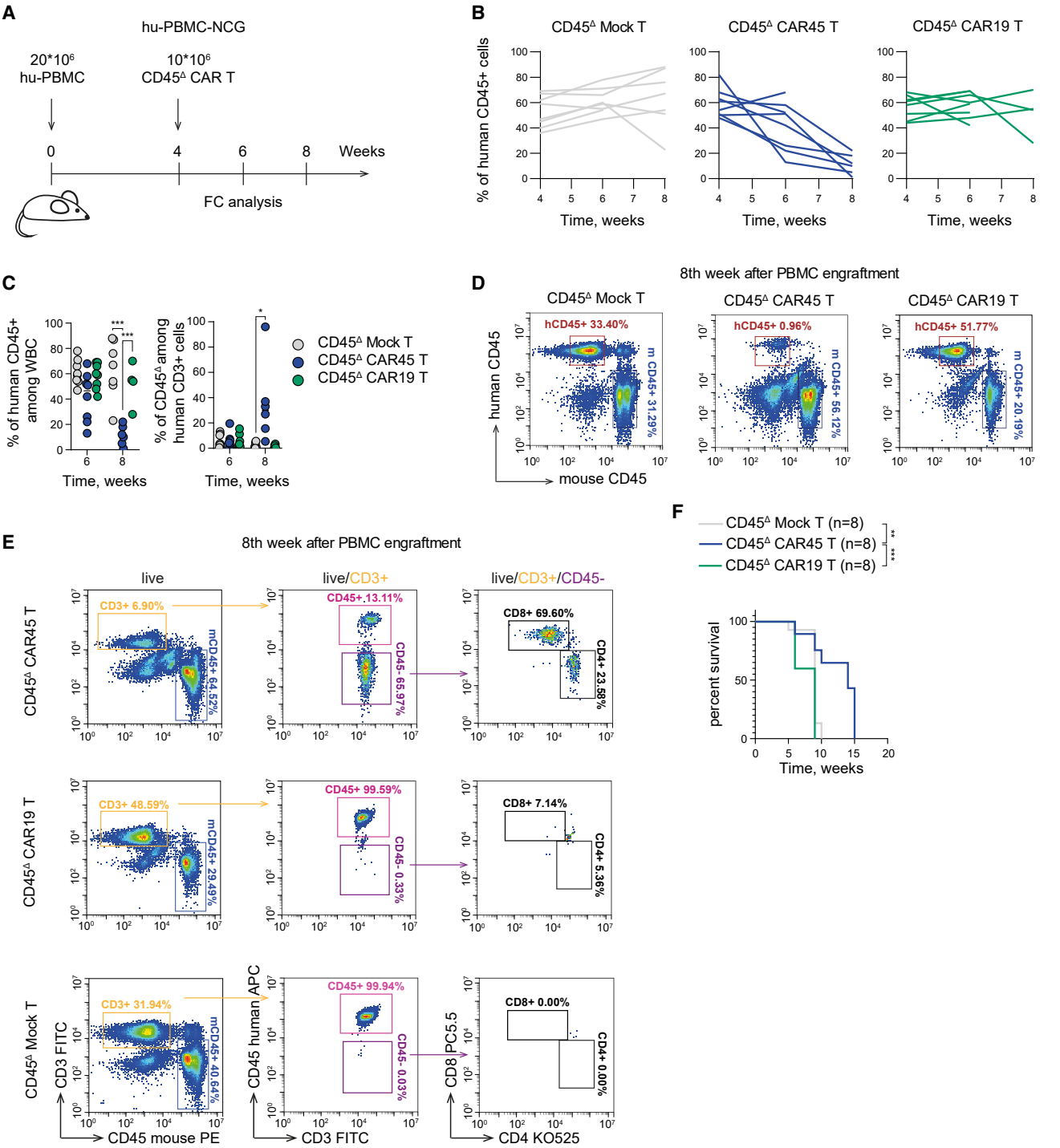

Figure 6. CD45Δ CAR45 T cells eliminate healthy autologous human PBMCs *in vivo*

(A) Schematic of the mouse model setup. NCG mice were subjected to i.v. infusion of 20 × 10^6 human PBMCs. On day 4 after PBMC engraftment, the animals were subjected to i.v. infusion of 10 × 10^6 CD45Δ CAR19, CD45Δ CAR45, and CD45Δ mock-transduced T cells. (B) Effects of CD45Δ CAR45 T cells on autologous human PBMCs *in vivo*. Hu-PBMC-NCG mouse chimerism was evaluated by flow cytometry on weeks 4, 6, and 8 after PBMC engraftment (as the percentage of circulating human CD45-positive cells). Each line represents an individual mouse. (C) Number and percentage of circulating $CD45^-/CD3^+$ human cells analyzed at weeks 6 and 8 of the experiment.

(legend continued on next page)

an ADC were recently released, and early clinical experience suggests that they have high potential as engraftment-facilitating agents.[47,48] However, monotherapy targeting CD117 might not provide sufficient immune suppression for the engraftment of allogeneic hematopoietic cells beyond the cohort of severe combined immune deficiency patients. The same is true for other potential immunotherapeutics targeting myeloid-associated antigens, as they will, by definition, spare the lymphoid compartments. To address these limitations, it has been suggested that anti-CD117 antibodies and similar myeloid-targeted agents can be combined with broadly immunosuppressive agents, including CD45-targeted agents,[49,50] to achieve better HSCT conditioning.

CD45, a common leukocyte antigen expressed by almost all nucleated white cells, including T cells, NK cells, and granulocytes, is a particularly attractive target for hematologic malignancies and HSCT for nonmalignant indications. The level of CD45 expression generally increases as the cells mature. CD45 targeting was pioneered by M. Brenner[16]; unfortunately, the naked antibody did not reach the late clinical trial stage. Alternatively, anti-CD45 radioconjugates have been developed primarily for treating leukemia and lymphoma patients.[51–53] Ample preclinical and early clinical evidence demonstrated that this approach could deliver high doses of radiation with high efficacy and limited direct toxicity.[54–56] Using radioconjugates has obvious limitations in cohorts of patients with nonmalignant disorders and in children, where long-term genotoxicity should be minimized. The use of an anti-CD45-based ADC was recently proposed as a nongenotoxic approach for patients with primary immune deficiency and constitutional bone marrow failure.[10,12,57] The results of this promising preclinical work are awaiting confirmation in human studies.

CD45 targeting by CAR T cells, however, has not been considered feasible for several reasons: (1) shared antigen expression between the target cells and CAR T cells may result in fratricide. Of note, naturally CD5-negative and CD7-negative T cells can be selected to produce CAR T cells of the relevant specificity, a phenomenon not described for CD45.[31,36,43] Based on this observation, gene-editing approaches to generate CD5- and CD7-specific CAR T cells have been developed to obviate fratricide. (2) Given the severe combined immune deficiency phenotype generated by human constitutional CD45 deficiency,[58] the idea that the removal of such an important molecule as CD45 would preserve T cell functionality seems counterintuitive. In addition, the importance of CD45 expression for T cells driven by synthetic CARs has not been clearly established.

In this study, we provide the first proof-of-concept demonstration of the generation and preclinical assessment of fratricide-resistant CAR T cells for targeting CD45-expressing human hematopoietic cells (referred to as CD45$^{\Delta}$ CAR45 T cells). We show that disruption of the CD45 gene by CRISPR-Cas9 and a CAR transduction protocol reliably yield a highly enriched population of gene-edited CD45$^{\Delta}$ CAR45 T and NK cells in the presence of the kinase inhibitor dasatinib. Dose and timing of the dasatinib treatment appear to play a critical role in balancing "fratricide" and target cell elimination. Disruption of the CD45 gene does not impair cytotoxicity and other functions of T cells. CD45$^{\Delta}$ CAR45 T cells specifically kill CD45^{+} acute myeloid leukemia (AML), T-cell acute lymphoblastic leukemia (T-ALL), and Mantle cell lymphoma (MCL) cell lines and primary hematopoietic stem and progenitor cells. Furthermore, CD45$^{\Delta}$ CAR45 T cells deplete AML cell lines as well as healthy donor PBMCs *in vivo* in mouse xenograft models. We observed the incomplete elimination of PBMCs engrafted in NCG mice, which could be explained by the limitations of the hu-PBMC engraftment model or, alternatively, by the experimental conditions (number of transferred cells or regimen of treatments), parameters deserving further optimization. The maximum allowable doses of CAR T cells were used in *in vivo* experiments to provide proof of principle that CD45$^{\Delta}$ CAR45 cells could be a robust and feasible alternative to other tumor-clearing CAR T cells. Harnessing the cytotoxic potential of CAR T cells while attenuating the toxic side effects of chemotherapy in the preconditioning step may offer a more balanced, safe, and effective "double-kill" immunotherapy. Our findings establish CD45 as a strong candidate target for CAR-mediated immunotherapy against leukemia and, at the same time, as a preconditioning strategy before HSCT. It is worth mentioning that an elegant alternative approach to targeting CD45 has recently been reported, using base editing of HSCs to generate a mutant CD45 that is resistant to recognition by the anti-CD45.[59]

There are several ways to further improve CD45$^{\Delta}$ CAR45 for clinical translation. This approach could be tested in the autologous setting or further developed with multiple gene edits into an allogeneic or even universal "off-the-shelf" product. Since long-term persistence is not the desired property of the CD45-targeting agent, safety switches; additional conditioning post CD45$^{\Delta}$ CAR45 T therapy; markers for antibody-mediated depletion; transient CAR expression via mRNA or, alternatively, adapter molecule-based CAR design; and other modification methods with demonstrated efficacy[60–64] could be considered. In addition to establishing the adequate dosing regimen of CAR T, we aim to enhance the complexity and precision of our experimental model system by adopting HSC-implanted mice, which more accurately reconstruct hematopoiesis without eliciting a GvHD reaction.

In summary, we have demonstrated proof of concept of gene-edited antihuman CD45 CAR T cells as a highly effective immunotherapeutic modality for leukemia, and we envision that this approach

Each dot represents an individual mouse. The *p* values were determined by multiple unpaired t tests. Nonsignificant values are not shown. (D) Representative dot plots of the chimerism analysis for the mice in (B) on week 8 of the experiment. Numbers indicate the percentages of human CD45 (hCD45) and mouse (mCD45) cells in the sample. (E) Gating strategy and representative dot plots of flow cytometry analysis of CAR T cell persistence at week 8 post injection. (F) Kaplan-Meier curve showing overall animal survival in each experimental group. The *p* values were determined by the log-rank Mantel-Cox test. Nonsignificant values are not shown. All data represent the mean ± SD. * indicates $p \leq 0.05$, ** indicates $p \leq 0.01$, *** indicates $p \leq 0.001$.

will enhance the curative potential of preconditioning regimens prior to allogeneic HSCT. For nonmalignant indications, it would provide the necessary immune suppression and create "space" for engraftment. In the case of hematologic malignancies, it would provide additional antileukemia activity. Alternatively, CAR45 could be used as an add-on antileukemia agent with a nonoverlapping toxicity profile and resistance mechanisms in cases of refractory leukemia.

MATERIALS AND METHODS

Flow cytometry analysis

A total of 3×10^5 cells were centrifuged ($300 \times g$, 5 min, room temperature [RT]) and resuspended in 100 μL of PBS. Surface antigens were stained with fluorescently labeled antibodies (Table S2) for 30 min at 4°C. The cells were washed once with 1 mL of cold PBS ($300 \times g$, 5 min, RT) and resuspended in 110 μL of cold PBS. Data were acquired using an ACEA NovoCyte 2060 flow cytometer (Agilent, USA). ACEA NovoExpress (Agilent, USA) was used for data analysis. For FACS, stained cells were acquired on an SH800 cell sorter (Sony, USA).

Cells and culture conditions

The HEK293T lentivirus packaging (Clontech, USA) and 293Vec-RD114 retrovirus packaging cell lines (BioVec Pharma, Canada) were cultured in DMEM (Gibco, USA) supplemented with 10% fetal bovine serum (FBS) (Gibco, USA), 100 U/mL penicillin (Gibco, USA), 100 μg/mL streptomycin (Gibco, USA), and 2 mM GlutaMAX (Gibco). The Jeko-1, Nalm-6, Jurkat, Raji, THP-1, K562, and Ramos cell lines were cultured in RPMI 1640 (Gibco, USA) supplemented with 10% FBS (Gibco, USA), 100 U/mL penicillin (Gibco, USA), 100 μg/mL streptomycin (Gibco, USA), and 2 mM GlutaMAX (Gibco). The lentivirus packaging HEK293T cell line was purchased from Clontech (USA). The Jeko-1, Nalm-6, Raji, THP-1, K562, Ramos, and Jurkat cell lines were purchased from ATCC (USA). The Jurkat NFAT Lucia reporter cell line was purchased from Invivogen (USA). Irradiated K562 feeder cells with 4-1BB and IL-21 surface expression were obtained as described previously.[65]

T cells from healthy donors were activated and cultured in TexMacs medium (Miltenyi, USA), supplemented with 12.5 ng/mL IL-7 (Miltenyi, USA) and 12.5 ng/mL IL-15 (Miltenyi, USA), or RPMI 1640 (Gibco, USA) medium supplemented with 100 U/mL IL-2 (Sci-Store, Russia). NK cells from healthy donors were cultured in TexMacs medium (Miltenyi, USA) supplemented with 10 U/mL IL-2 (Sci-Store, Russia). All cytotoxicity assays were performed in TexMacs medium with IL-7 and IL-15 or RPMI 1640 medium with IL-2 (Sci-Store, Russia). The Jeko-1, Nalm-6, Raji, THP-1, K562, Ramos, and Jurkat cell lines were modified by lentiviral transduction to induce stable ffluc or green fluorescent protein (GFP) expression. For the Incucyte assay, THP-1 or Jeko-1 cells were transduced with Incucyte NucLight Red Lentivirus Reagent (EF-1 Alpha, Puro) (Sartorius, USA). All cell lines were repeatedly tested for the presence of mycoplasma contamination with a MycoReport Mycoplasma Detection Kit (Evrogen, Russia).

Isolation of primary human PBMCs

Human PBMCs were isolated from the blood of healthy donors by gradient density centrifugation on Ficoll-Paque (GE Healthcare, USA) according to a standard protocol approved by the local ethics committee of the Dmitry Rogachev National Medical Research Center of Pediatric Hematology, Oncology, and Immunology. All participants provided informed consent. T cells were isolated from human PBMCs with an Untouched human T cell isolation kit (Invitrogen, USA) and activated with Dynabeads Human T-Activator CD3/CD28 beads (Gibco, USA) at a 1:1 ratio for 24 h. NK cells were isolated from PBMCs with an NK cell isolation kit (Miltenyi, USA). NK cells were mixed with irradiated K562 feeder cells at a 1:10 ratio for 5 days, and on day 5, transduction was performed.

Chimeric antigen receptors

The nucleotide sequence of CAR45 consists of the following parts: anti-CD45 scFv (from CD45 antibody clone BC8),[41] the human IgG4 hinge region, the CD28 transmembrane domain, CD28 and OX-40 co-stimulatory domains, and the CD3ζ signaling domain. A synthetic anti-CD45 scFv gene (GeneCust, France) was cloned and inserted into the pLV2 lentiviral vector (Clontech, USA) and pMM25b retroviral vector (a gift from Dr. M. Mamonkin). The CAR19 nucleotide sequences were obtained as described previously[66] and cloned and inserted into the pLV2 and pMM25b vectors. All sequences were validated by Sanger sequencing (Evrogen, Russia).

Transduction of T cells and NK cells with pseudoviral particles

Lentiviral particles containing CAR45 and CAR19 were produced by polyethylenimine-mediated co-transfection (Sigma, USA) of HEK293T cells with the corresponding lentiviral CAR plasmids and the packaging plasmids pCMV VSV-G, pRSV-REV, and pMDLg-pRRE (a gift from Dr. I. Verma). Supernatants were collected at 48 h post transfection and purified by two rounds of centrifugation (first—$300 \times g$, 5 min, RT; second—$4{,}500 \times g$, 5 min, RT). On the second day after isolation, 1×10^6/mL activated T cells were resuspended in TexMacs medium and mixed with lentiviral supernatants and 13 μg/mL Polybrene (Sigma, USA). Dasatinib (STEMCELL, Canada) was diluted in pure dimethyl sulfoxide up to 10 mM, aliquoted, and stored frozen at −20°C. Prior to transduction, dasatinib was added to cells at 50 nM concentration. The cells were centrifuged at $1{,}200 \times g$ for 90 min at 32°C and incubated at 37°C with 5% CO_2 for 18 h. To avoid fratricide during the manufacturing process, the culture medium with 50 nM dasatinib was changed on the day after transduction and every 3 or 4 days to maintain the cells at a density of 2.0×10^6 cells/mL. CAR T cells were cultivated up to 14–21 days in culture and were used without cryopreservation.

Retroviral particles containing CAR45 or CAR19 were produced by polyethylenimine-mediated transfection of 293Vec-RD114 cells. Supernatants containing the virus were collected at 48 h post transfection and purified by two rounds of centrifugation (first—$300 \times g$, 5 min, RT; second—$4{,}500 \times g$, 5 min, RT). A total of 0.5×10^6 NK cells were resuspended in TexMacs medium with 100 nM dasatinib on the fifth day after isolation. Retroviral supernatants were mixed

with 10 μg/mL Vectofusin-1 (Miltenyi, USA) and added to NK cell suspensions. The cells were centrifuged at 400 × *g* for 2 h at 37°C and incubated at 37°C with 5% CO_2 for 48 h. The culture medium supplemented with 50 nM dasatinib was changed on the second day after transduction and every 3 or 4 days to maintain cells at a density of 2.0 × 10^6 cells/mL. CAR NK cells were cultivated up to 14–21 days in culture and were used without cryopreservation.

Target cell modification

To obtain reporter cells, Jeko-1, Nalm-6, Nalm-6 CD19$^{\Delta}$, Raji, THP-1, K562, Ramos, and Jurkat cells were transduced to express the fluorescent protein GFP and the reporter protein ffluc simultaneously. The reporter cell lines were stained with anti-human CD45 and anti-human CD19 antibodies and analyzed by flow cytometry on an ACEA NovoCyte 2060 (Agilent, USA). ACEA NovoExpress (Agilent, USA) was used for data analysis.

Gene knockout in cells

The procedure was performed by electroporation with a 4D-Nucleofector device (Lonza, Switzerland) using the CRISPR-Cas9 system and the P3 Primary Cell 4D-Nucleofector X Kit L (Lonza, Switzerland). Oligonucleotides for gRNAs were selected by Crispor (Tefor Infrastructure, France) algorithms and synthesized by Evrogen, Russia (Figure S1A). Three gRNAs specific to the human CD45 gene (GGATTTGTGGCTTAAACTCT, GGGTTTAAGCCA CAAATACA, and GGCACACTTATACTCATGTT) were evaluated for gene editing efficiency in combination and/or individually. Two gRNAs (GGCTCATGAGCTTCCCGGAA and GGGCGGGGACTC CCGAGACC) were utilized for CD19 gene knockout as described previously.[67] Short nucleotide sequences were used for transcription according to the HiScribe Quick T7 High Yield RNA Synthesis Kit (NEB, UK) protocol. The resulting gRNAs were purified using the AMPure XP kit and treated with DNase I (NEB, UK). Concentration was evaluated on a Qubit system (Thermo Fisher Scientific, USA). For electroporation, 2 μg of gRNA was mixed with 3.3 μL of Spy Cas9 NLS (NEB, UK) and incubated for 30 min at RT. For CD45 knockout, T and CAR T cells (on the third day after isolation and the second day after transduction) or NK cells and CAR NK cells (on the seventh day after isolation and the second day after transduction) were washed twice with PBS (300 × *g*, 5 min, RT), resuspended in 100 μL of electroporation buffer, and mixed with the gRNA + Cas9 mix according to the P3 protocol for the Primary Cell 4D-Nucleofector XL Kit. For CD19 knockout, Nalm-6 cells were prepared similarly. Electroporation was performed using the DN-100 program for NK cells and the EH100 program for T cells and Nalm-6 cells. The survival and proliferation rates were evaluated by trypan blue 0.04% (Bio-Rad, USA) staining every 2 days using a TC20 cell counter (Bio-Rad, USA). Briefly, cells were resuspended in culture medium, and 10 μL of the suspension was mixed with 10 μL of trypan blue. Ten microliters of the mixture was injected into a counting slide (Bio-Rad, USA) and analyzed on a cell counter. The knockout efficiency was assessed on the fifth day after electroporation by flow cytometry on an ACEA NovoCyte 2060 (Agilent, USA). ACEA NovoExpress (Agilent, USA) was used for data analysis. For Nalm-6 cells, the knockout population was enriched by FACS on an SH800S cell sorter (Sony, USA).

Off-target analysis for CD45 gRNAs

A total of 183 potential off-target sites were identified with the use of the CRISPOR software tool for off-target prediction. We selected all predicted off-target sites with a CFD (cutting frequency determination) score $\geq$0.21 (n = 20) and the off-target sites predicted within exons independent of the CFD (N = 5). For each of the selected loci, we designed a pair of primers using Primer-BLAST. A pair of primers flanking the gRNA target in *PTPRC* was added as a positive control. These primers were pooled and used for multiplex PCR with genomic DNA isolated from cells electroporated with Cas9/gRNA ribonucleoprotein (RNP) or with pure Cas9 without gRNA as a negative control. Cells were collected at 4, 8, and 16 h after electroporation. Six multiplex amplicons were ligated to Illumina TruSeq adapters using the NEBNext Ultra II DNA Library Prep Kit for Illumina,[5] pooled, and sequenced on an Illumina NextSeq 550 (paired-end 100 + 100), resulting in 2.1–2.8 million raw sequencing reads per library. The reads were preprocessed with TrimGalore v.0.6.4 and mapped to the human genome (Hg38) using Bowtie 2 v.2.3.5.1. Metrics for target regions were collected with GATK v.4.1.4.1 CollectTargeted PcrMetrics. The percentage of insertions and deletions was calculated in R with the GenomicAlignments package for each amplicon separately in cells treated with Cas9 with and without gRNA at different time points.

Sanger sequencing

Genomic DNA (gDNA) for T and CD45$^{\Delta}$ T cells was obtained with an ExtractDNA Blood & Cells Kit (Evrogen, Russia) on the second day after knockout. The BigDye Direct Sanger Sequencing Kit (Thermo Fisher Scientific, USA) and GCAAAGAGGACCCT TACAGTAT and AGATACAGATAGACATTGCTTTC primers were utilized for the subsequent analysis according to the manufacturer's instructions. Sequencing reactions were analyzed on a 3500 genetic analyzer (Thermo Fisher Scientific, USA).

Western blotting

Cell pellets of 1 × 10^5 T or CD45$^{\Delta}$ T cells were lysed with RIPA lysis buffer (50 mM Tris HCl, 150 mM NaCl, 1.0% [v/v] NP-40, 0.5% [w/v] sodium deoxycholate, 1.0 mM EDTA, 0.1% [w/v] SDS, and 0.01% [w/v] sodium azide [pH 7.4]). Cell lysates were mixed with 2× sample buffer (125 mM Tris HCl [pH 6.8], 4% [w/v] SDS, 20% [v/v] glycerol, 100 mM DTT, 0.01% bromophenol blue) and heated at 90°C for 10 min. Samples were separated by SDS-PAGE on a 12.5% polyacrylamide gel, transferred to a nitrocellulose membrane (Bio-Rad, USA), and incubated with a recombinant anti-human CD45 primary antibody and a horseradish peroxidase (HRP)-conjugated goat anti-rabbit IgG secondary antibody according to the manufacturers' protocols. An HRP-conjugated anti-human GAPDH antibody was used as a positive control. The presence of CD45 and GAPDH was assessed on a VersaDoc 4000 MP imaging system (Bio-Rad, USA) using an Enhanced Chemiluminescence kit (Bio-Rad, USA).

Confocal microscopy

Jurkat T cells or CD45$^{\Delta}$ Jurkat T cells were plated on poly-L-lysine-covered coverslips and centrifuged (100 × *g*, 10 min, RT). The attached cells were fixed in 4% formalin for 1 h at RT and stained with anti-human CD45 antibodies against extracellular and intracellular CD45. Confocal images were captured using an Axio Observer Z1 microscope (Carl Zeiss AG, Germany) with a Yokogawa spinning disc confocal device CSU-X1 (Yokogawa Corp. of America, USA).

CAR T cell expansion assay

A total of 1×10^5 CD45$^{\Delta}$ CAR45 T cells or CD45$^{\Delta}$ CAR19 T cells were plated in 24-well plates in TexMacs medium supplemented with IL-7/IL-15 and with or without 50 nM dasatinib (STEMCELL, Canada). Cell number and viability were assessed every 2 days for 2 weeks by flow cytometry on an ACEA NovoCyte 2060 (Agilent, USA). ACEA NovoExpress (Agilent, USA) was used for data analysis.

Detection of proinflammatory cytokines

A total of 5×10^4 Ramos cells (target cells) were mixed with 2.5×10^5 T or CD45$^{\Delta}$ T cells (effector cells) on the 8th to the16th day after knockout of CD45 (E:T ratio 5:1) in TexMacs medium supplemented with IL-7, IL-15, and 1 nM blinatumomab (Amgen, USA). Wells containing only effector cells were used as negative controls. Cells were incubated at 37°C with 5% CO_2 for 24 h. The supernatant was separated from the cells by centrifugation (4°C, 300 × *g*, 5 min) and stored at −20°C before use. The concentrations of the cytokines IL-2 and IFN-γ were measured using ELISA-based kits (Vector-Best, Russia) according to the manufacturer's instructions. Data were analyzed with a Varioskan Flash instrument (Thermo Fisher Scientific, USA) using SkanIt RE for Varioskan Flash 2.4.5 (Thermo Fisher Scientific, USA).

A total of 5×10^3, 1×10^4, 2.5×10^4, or 5×10^4 THP-1 or Jeko-1 cells (target cells) were mixed with 5×10^4 CD45$^{\Delta}$ CAR45 T cells, CD45$^{\Delta}$ CAR19 T cells, or CD45$^{\Delta}$ T cells (effector cells) on the 10th day after CD45 knockout (E:T ratios 10:1, 5:1, 2:1, and 1:1) in RPMI 1640 medium. Wells containing only effector cells were used as negative controls. The cells were incubated at 37°C with 5% CO_2 for 24 h. The supernatant was separated from the cells by centrifugation (4°C, 300 × *g*, 5 min) and stored at −20°C before use. The concentrations of the cytokines IL-2 and IFN-γ were measured using ELISA-based kits (Vector-Best, Russia) according to the manufacturer's instructions. Data were analyzed with a Varioskan Flash instrument (Thermo Fisher Scientific, USA) using SkanIt RE for Varioskan Flash 2.4.5 (Thermo Fisher Scientific, USA).

T and CD45$^{\Delta}$ T cell cytotoxicity assay

A total of 5×10^4 Ramos cells expressing GFP (target cells) were mixed with 5×10^4 T or CD45$^{\Delta}$ T cells (effector cells) (E:T ratio 1:1) in TexMacs medium supplemented with IL-7, IL-15, and 1 nM blinatumomab. Wells with target cells only were used as negative controls. The cells were incubated at 37°C with 5% CO_2 for 24 h and were washed twice with PBS (Gibco, USA) (RT, 300 × *g*, 5 min). The results were evaluated by flow cytometry on an ACEA NovoCyte 2060 (Agilent, USA). ACEA NovoExpress (Agilent, USA) was used for data analysis.

Cytotoxicity assays of CAR T cells and CAR NK cells

Tumor cells

A total of 1×10^4, 2×10^4, or 5×10^4 CD19^{D} Nalm-6, Nalm-6, Raji, Jeko-1, Jurkat, THP-1, or Ramos cells (target cells) were mixed with 5×10^4 CD45$^{\Delta}$ CAR45 T cells, CAR45 T cells, CD45$^{\Delta}$ CAR19 T cells, CAR19 T cells, or T cells (effector cells) on the 8th-16th days after knockout of CD45 (E:T ratios were 5:1, 2.5:1, and 1:1). Wells containing only target cells were used as negative controls for cytotoxicity. Wells containing only effector cells were used as positive controls for viability. The cells were incubated at 37°C with 5% CO_2 for 24 h and washed twice with PBS (Gibco, USA) (300 × *g*, 5 min, RT). The results were evaluated by flow cytometry on an ACEA NovoCyte 2060 (Agilent, USA). ACEA NovoExpress (Agilent, USA) was used for data analysis.

Incucyte killing assay

For the Incucyte killing assay, 3×10^4 red-fluorescent THP-1 or Jeko-1 cells (target cells) were mixed with 9×10^4 CD45$^{\Delta}$ CAR45 T cells, CAR45 T cells, CD45$^{\Delta}$ CAR19 T cells, CAR19 T cells, or T cells (effector cells) on the 8th-16th days after knockout (E:T ratio was 3:1) in TexMacs medium (Miltenyi, USA) and incubated at 37°C with 5% CO_2 for 48 h. Wells containing only target cells were used as negative controls. Changes in fluorescence were monitored every 2 h using the Incucyte Live-Cell analysis system (Essen BioScience, USA). To determine the cytolytic activity of effector cells, the area under the curve (AUC) was calculated.

T cells and PBMCs

A total of 3×10^4 T cells or PBMCs (target cells) were mixed with CD45$^{\Delta}$ CAR19 T cells, CD45$^{\Delta}$ CAR45 T cells, or CD45$^{\Delta}$ T cells (E:T ratio 1:5, 1:2, 1:1, and 5:1) or CD45$^{\Delta}$ CAR45 NK cells, CAR45 NK cells, or NK cells (effector cells) on the 8th-16th days after CD45 knockout (E:T ratios 5:1, 1:1, and 1:2). Prior to the experiment, target T cells and PBMCs were stained with 5 μM carboxyfluorescein succinimidyl ester (CFSE) (Invitrogen, USA) according to the manufacturer's protocol. Wells containing only target or only effector cells were used as negative controls. For the CAR T cell experiment, the cells were incubated at 37°C with 5% CO_2 for 24 h. For the CAR NK cell experiment, the cells were incubated at 37°C with 5% CO_2 for 4 and 24 h. One hundred microliters of cell suspension from each well was stained with anti-human CD45 (anti-human CD3 for NK cell experiments) according to the manufacturer's instructions and washed twice with PBS (Gibco, USA) (300 × *g*, 5 min, 4°C). The results were evaluated by flow cytometry using ACEA NovoCyte 2060 (Agilent, USA). ACEA NovoExpress (Agilent, USA) was used for data analysis. The percentage of cell counts was normalized to the starting cell number.

PBMCs

PBMCs ($3 \times 10^{5,}$ target cells) were mixed with CD45$^{\Delta}$ CAR45 T cells or CD45$^{\Delta}$ T cells (E:T ratio 1:3) on the 8th-16th days after CD45 knockout. Wells containing only PBMCs or only effector cells with 50 nM

dasatinib were used as negative controls. For the CAR T cell experiment, the cells were incubated at 37°C with 5% CO_2 for 72 h. One hundred microliters of cell suspension from each well was stained with anti-human CD45 according to the manufacturer's instructions and washed twice with PBS (Gibco, USA) (300 × *g*, 5 min, 4°C). The results were evaluated by flow cytometry using ACEA NovoCyte 2060 (Agilent, USA). ACEA NovoExpress (Agilent, USA) was used for data analysis.

BM cells

A total of 3×10^5 BM cells (target cells) were mixed with $CD45^{\Delta}$ CAR45 T cells or $CD45^{\Delta}$ T cells (E:T ratio 1:3) on the 8th-16th days after CD45 knockout. Wells containing only BM cells or supplemented with 50 nM dasatinib were used as negative controls. For the CAR T cell experiment, the cells were incubated at 37°C with 5% CO_2 for 24, 48, and 72 h. One hundred microliters of cell suspension from each well was stained with anti-human CD45, CD33, CD3, CD56, CD16, CD19, and 7-AAD according to the manufacturer's instructions and washed twice with PBS (Gibco, USA) (300 × *g*, 5 min, 4°C). The results were evaluated by flow cytometry using ACEA NovoCyte 2060 (Agilent, USA). ACEA NovoExpress (Agilent, USA) was used for data analysis.

Intracellular detection of proinflammatory cytokines

A total of 3×10^5 $CD45^{\Delta}$ T cells (from two healthy donors) and T cells (from two healthy donors) (effector cells) were mixed with Dynabeads Human T Activator CD3/CD28 (Thermo Fisher Scientific, USA) on the 8th-16th days after knockout of CD45 (E:beads ratio was 1:1) in complete RPMI 1640 (Gibco, USA) medium and incubated at 37°C with 5% CO_2 for 18 h. Positive control wells containing only effector cells were activated with 40 nM phorbol 12-myristate 13-acetate (PMA) (Invitrogen, USA) and 1 μM ionomycin (Invitrogen, USA) for 3 h. Wells with untreated effector cells only served as negative controls. After incubation, experimental and control wells were mixed with 10 μg/mL brefeldin A (Sigma, USA) and incubated at 37°C with 5% CO_2 for 3 h. The beads were removed with a DynaMag (Thermo Fisher Scientific), and the cells were washed with PBS (500 × *g*, 5 min, RT). The cells were blocked with 5% FBS (Gibco, USA); stained with anti-human CD45, anti-human CD4, and anti-human CD8a for 15 min at RT; washed with PBS (500 × *g*, 5 min, RT); and fixed with 2% paraformaldehyde (Thermo Fisher Scientific, USA) at 4°C for 20 min. After fixation, the cells were washed with 0.2% saponin (Merck, Germany) in PBS (500 × *g*, 5 min, RT), blocked with 5% FBS (Gibco, USA), stained with anti-human IFN-γ and anti-human IL-2 antibodies for 40 min at RT in 0.2% saponin (Merck, Germany) in PBS (Gibco, USA), and washed twice with PBS (500 × *g*, 5 min, RT). The results were evaluated by flow cytometry using ACEA NovoCyte 2060 (Agilent, USA). Data were analyzed by ACEA NovoExpress software (Agilent, USA). ACEA NovoExpress (Agilent, USA) was used for data analysis. The antibodies used are described in Table S2.

In vivo study

Animals were housed under specific-pathogen-free conditions in the accredited IBCh animal breeding facility, which is accredited at the international level by AAALACi (the Unique Research Unit Bio-Model of the IBCh, RAS; the Bioresource Collection–Collection of SPF-Laboratory Rodents for Fundamental, Biomedical and Pharmacological Studies, no. 075-15-2021-1067). Six- to eight-week-old female and male NOD.Cg-*Prkdc*^{scid}*Il2rg*^{em1Smoc} (NCG) mice with an average weight of 21–24 g were used for the experiments.

In vivo *CAR19 and CD45*$^{\Delta}$ *CAR19 T cell activity study*

Tumors were engrafted by inoculating 1×10^6 Nalm-6 cells expressing ffluc and GFP i.v. in 100 μL of PBS (Gibco, USA). Mice were randomly assigned to two experimental groups and one control group. Tumor-bearing mice were subjected to i.v. injection of 2×10^6 $CD45^{\Delta}$ CAR19 T cells, CAR19 T cells (experimental groups), or mock T cells (control group) on the seventh day after tumor engraftment. Tumors were observed weekly for 5 weeks using an IVIS Spectrum *in vivo* imaging system (PerkinElmer, USA) after intraperitoneal (i.p.) injection of D-luciferin (GoldBio, USA) according to the manufacturer's instructions.

In vivo *CAR45 and CD45*$^{\Delta}$ *CAR45 T cell activity study*

Tumors were engrafted via i.v. inoculation of 2×10^6 THP-1 cells expressing ffluc and GFP in 100 μL of PBS (Gibco, USA). Mice were randomly assigned to four experimental groups and one control group. Tumor-bearing mice were subjected to i.v. injection of 5×10^6 $CD45^{\Delta}$ CAR45 T cells, CAR45 T cells (experimental groups), or mock T cells (control group) on the 3rd or 7th day after tumor inoculation. Mice that received therapy on the 7th day were injected twice with 2.5×10^6 $CD45^{\Delta}$ CAR45 T cells and CAR45 T cells on the 13th and 20th days. Tumors were observed weekly for 11 weeks, starting on the 6th day after THP-1 injection, using an IVIS Spectrum *in vivo* imaging system (PerkinElmer, USA) after i.p. injection of D-luciferin (GoldBio, USA) according to the manufacturer's instructions.

In vivo *CAR45 and CD45*$^{\Delta}$ *CAR45 T cell activity study in hu-PBMC-NCG mice*

Mice were subjected to i.v. injection of 20×10^6 PBMCs from donor 1. After 2 weeks, the mice were randomly assigned to experimental and control groups and were injected with 10×10^6 $CD45^{\Delta}$ CAR45 T cells or $CD45^{\Delta}$ CAR19 T cells derived from donor 1. For flow cytometry analysis, blood samples from the retroorbital sinus were collected. Human $CD45^{+}$ cell and CAR T cell counts were monitored by staining of blood samples with antihuman antibodies against CD45, CD3, and IgG (Table S2), and the results were acquired with a CytoFLEX flow cytometer (Beckman Coulter, USA) in the second, fourth, and eighth weeks after PBMC injection.

Statistics

Statistical analysis was performed using GraphPad Prism 8.0 (GraphPad, USA). Each figure legend denotes the statistical test used. Mean values are plotted as bar graphs, and error bars indicate the standard deviation (SD) unless otherwise stated. ANOVA multiple-comparison *p* values were calculated using Tukey's multiple-comparisons test. The t test multiple-comparison *p* values were calculated

using the two-stage step-up (Benjamini, Krieger, and Yekutieli) method. All t tests were two-tailed unless otherwise indicated.

DATA AND CODE AVAILABILITY

The main data supporting the results in this study are available within the paper and the supplemental information. All data generated in this study are available from the corresponding authors on reasonable request.

SUPPLEMENTAL INFORMATION

Supplemental information can be found online at https://doi.org/10.1016/j.omton.2024.200843.

ACKNOWLEDGMENTS

We thank Dr. Mamonkin for fruitful discussions and scientific advice and for his support of this article. P.W. was partially supported by the NIH (R35GM139643). H.Z. was partially supported by the National Natural Science Foundation of China (grant 82261138553). V.M.S., D.V.V., and A.G.G. were partially supported by RSF 23-44-00043. The authors thank the charitable foundation Science to Children for constant support of cellular immunotherapy project. All studies were conducted in accordance with protocols approved by the local ethics committee of the Dmitry Rogachev National Medical Research Center of Pediatric Hematology, Oncology, and Immunology (decision on 2018.01.18) and the IBCh RAS Institutional Animal Care and Use Committee.

AUTHOR CONTRIBUTIONS

V.M.S., D.V.V., D.S.O., W.W., Y.H., D.E.P., M.S.F., E.A.M., E.A.K., D.Z., I.Z.M., A.S.C., Y.P.R., and A.V.S. performed experiments and analyzed and interpreted data; L.C., Z.M., H.Z., J.X., A.G.G., P.W., I.Z.M., G.B.T., Y.P.R., A.G.G., M.A.M., and A.V.S. analyzed and interpreted data and revised the manuscript; P.W., M.A.M., and A.V.S. designed the research, analyzed and interpreted data, and wrote the paper.

DECLARATION OF INTERESTS

The authors declare no competing interests.

REFERENCES

1. Zeiser, R., and Blazar, B.R. (2017). Acute Graft-versus-Host Disease - Biologic Process, Prevention, and Therapy. N. Engl. J. Med. *377*, 2167–2179.
2. Yao, S., Hahn, T., Zhang, Y., Haven, D., Senneka, M., Dunford, L., Parsons, S., Confer, D., and McCarthy, P.L. (2013). Unrelated donor allogeneic hematopoietic cell transplantation is underused as a curative therapy in eligible patients from the United States. Biol. Blood Marrow Transplant. *19*, 1459–1464.
3. Ebens, C.L., MacMillan, M.L., and Wagner, J.E. (2017). Hematopoietic cell transplantation in Fanconi anemia: current evidence, challenges and recommendations. Expert Rev. Hematol. *10*, 81–97.
4. Giardino, S., de Latour, R.P., Aljurf, M., Eikema, D.J., Bosman, P., Bertrand, Y., Tbakhi, A., Holter, W., Bornhäuser, M., Rössig, C., et al. (2020). Outcome of patients with Fanconi anemia developing myelodysplasia and acute leukemia who received allogeneic hematopoietic stem cell transplantation: A retrospective analysis on behalf of EBMT group. Am. J. Hematol. *95*, 809–816.
5. Slack, J., Albert, M.H., Balashov, D., Belohradsky, B.H., Bertaina, A., Bleesing, J., Booth, C., Buechner, J., Buckley, R.H., Ouachée-Chardin, M., et al. (2018). Outcome of hematopoietic cell transplantation for DNA double-strand break repair disorders. J. Allergy Clin. Immunol. *141*, 322–328.e10.
6. Matthews, D.C., Martin, P.J., Nourigat, C., Appelbaum, F.R., Fisher, D.R., and Bernstein, I.D. (1999). Marrow ablative and immunosuppressive effects of 131I-anti-CD45 antibody in congenic and H2-mismatched murine transplant models. Blood *93*, 737–745.
7. Ruffner, K.L., Martin, P.J., Hussell, S., Nourigat, C., Fisher, D.R., Bernstein, I.D., and Matthews, D.C. (2001). Immunosuppressive effects of (131)I-anti-CD45 antibody in unsensitized and donor antigen-presensitized H2-matched, minor antigen-mismatched murine transplant models. Cancer Res. *61*, 5126–5131.
8. Orozco, J.J., Kenoyer, A., Balkin, E.R., Gooley, T.A., Hamlin, D.K., Wilbur, D.S., Hylarides, M.D., Frost, S.H.L., Mawad, R., O'Donnell, P., et al. (2016). Anti-CD45 radioimmunotherapy without TBI before transplantation facilitates persistent haploidentical donor engraftment. Blood *127*, 352–359.
9. Tuazon, S.A., Sandmaier, B.M., Gooley, T.A., Fisher, D.R., Holmberg, L.A., Becker, P.S., Lundberg, S.J., Orozco, J.J., Gopal, A.K., Till, B.G., et al. (2021). (90)Y-labeled anti-CD45 antibody allogeneic hematopoietic cell transplantation for high-risk multiple myeloma. Bone Marrow Transplant. *56*, 202–209.
10. Palchaudhuri, R., Saez, B., Hoggatt, J., Schajnovitz, A., Sykes, D.B., Tate, T.A., Czechowicz, A., Kfoury, Y., Ruchika, F., Rossi, D.J., et al. (2016). Non-genotoxic conditioning for hematopoietic stem cell transplantation using a hematopoietic-cell-specific internalizing immunotoxin. Nat. Biotechnol. *34*, 738–745.
11. Czechowicz, A., Palchaudhuri, R., Scheck, A., Hu, Y., Hoggatt, J., Saez, B., Pang, W.W., Mansour, M.K., Tate, T.A., Chan, Y.Y., et al. (2019). Selective hematopoietic stem cell ablation using CD117-antibody-drug-conjugates enables safe and effective transplantation with immunity preservation. Nat. Commun. *10*, 617.
12. Castiello, M.C., Bosticardo, M., Sacchetti, N., Calzoni, E., Fontana, E., Yamazaki, Y., Draghici, E., Corsino, C., Bortolomai, I., Sereni, L., et al. (2021). Efficacy and safety of anti-CD45-saporin as conditioning agent for RAG deficiency. J. Allergy Clin. Immunol. *147*, 309–320.e6.
13. Saha, A., Hyzy, S., Lamothe, T., Hammond, K., Clark, N., Lanieri, L., Bhattarai, P., Palchaudhuri, R., Gillard, G.O., Proctor, J., et al. (2022). A CD45-targeted antibody-drug conjugate successfully conditions for allogeneic hematopoietic stem cell transplantation in mice. Blood *139*, 1743–1759.
14. Czechowicz, A., Kraft, D., Weissman, I.L., and Bhattacharya, D. (2007). Efficient transplantation via antibody-based clearance of hematopoietic stem cell niches. Science *318*, 1296–1299.
15. Xue, X., Pech, N.K., Shelley, W.C., Srour, E.F., Yoder, M.C., and Dinauer, M.C. (2010). Antibody targeting KIT as pretransplantation conditioning in immunocompetent mice. Blood *116*, 5419–5422.
16. Wulf, G.G., Luo, K.L., Goodell, M.A., and Brenner, M.K. (2003). Anti-CD45-mediated cytoreduction to facilitate allogeneic stem cell transplantation. Blood *101*, 2434–2439.
17. Pang, W.W., Czechowicz, A., Logan, A.C., Bhardwaj, R., Poyser, J., Park, C.Y., Weissman, I.L., and Shizuru, J.A. (2019). Anti-CD117 antibody depletes normal and myelodysplastic syndrome human hematopoietic stem cells in xenografted mice. Blood *133*, 2069–2078.
18. Arai, Y., Choi, U., Corsino, C.I., Koontz, S.M., Tajima, M., Sweeney, C.L., Black, M.A., Feldman, S.A., Dinauer, M.C., and Malech, H.L. (2018). Myeloid Conditioning with c-kit-Targeted CAR-T Cells Enables Donor Stem Cell Engraftment. Mol. Ther. *26*, 1181–1197.
19. Myburgh, R., Kiefer, J.D., Russkamp, N.F., Magnani, C.F., Nuñez, N., Simonis, A., Pfister, S., Wilk, C.M., McHugh, D., Friemel, J., et al. (2020). Anti-human CD117 CAR T-cells efficiently eliminate healthy and malignant CD117-expressing hematopoietic cells. Leukemia *34*, 2688–2703.
20. Tambaro, F.P., Singh, H., Jones, E., Rytting, M., Mahadeo, K.M., Thompson, P., Daver, N., DiNardo, C., Kadia, T., Garcia-Manero, G., et al. (2021). Autologous CD33-CAR-T cells for treatment of relapsed/refractory acute myelogenous leukemia. Leukemia *35*, 3282–3286.
21. Sugita, M., Galetto, R., Zong, H., Ewing-Crystal, N., Trujillo-Alonso, V., Mencia-Trinchant, N., Yip, W., Filipe, S., Lebuhotel, C., Gouble, A., et al. (2022). Allogeneic TCRαβ deficient CAR T-cells targeting CD123 in acute myeloid leukemia. Nat. Commun. *13*, 2227.

22. El Khawanky, N., Hughes, A., Yu, W., Myburgh, R., Matschulla, T., Taromi, S., Aumann, K., Clarson, J., Vinnakota, J.M., Shoumariyeh, K., et al. (2021). Demethylating therapy increases anti-CD123 CAR T cell cytotoxicity against acute myeloid leukemia. Nat. Commun. *12*, 6436.

23. Dahlke, M.H., Larsen, S.R., Rasko, J.E.J., and Schlitt, H.J. (2004). The biology of CD45 and its use as a therapeutic target. Leuk. Lymphoma *45*, 229–236.

24. Caldwell, C.W., and Patterson, W.P. (1991). Relationship between CD45 antigen expression and putative stages of differentiation in B-cell malignancies. Am. J. Hematol. *36*, 111–115.

25. Ratei, R., Sperling, C., Karawajew, L., Schott, G., Schrappe, M., Harbott, J., Riehm, H., and Ludwig, W.D. (1998). Immunophenotype and clinical characteristics of CD45-negative and CD45-positive childhood acute lymphoblastic leukemia. Ann. Hematol. *77*, 107–114.

26. Nakamura, A., Tsurusawa, M., Kato, A., Taga, T., Hatae, Y., Miyake, M., Mimaya, J., Onodera, N., Watanabe, A., Watanabe, T., et al. (2001). Prognostic impact of CD45 antigen expression in high-risk, childhood B-cell precursor acute lymphoblastic leukemia. Leuk. Lymphoma *42*, 393–398.

27. Heo, S.K., Noh, E.K., Ju, L.J., Sung, J.Y., Jeong, Y.K., Cheon, J., Koh, S.J., Min, Y.J., Choi, Y., and Jo, J.C. (2020). CD45(dim)CD34(+)CD38(-)CD133(+) cells have the potential as leukemic stem cells in acute myeloid leukemia. BMC Cancer *20*, 285.

28. Brenner, M.K., Wulf, G.G., Rill, D.R., Luo, K.L., Goodell, M.A., Mei, Z., Kuehnle, I., Brown, M.P., Pule, M., Heslop, H.E., and Krance, R.A. (2003). Complement-fixing CD45 monoclonal antibodies to facilitate stem cell transplantation in mouse and man. Ann. N. Y. Acad. Sci. *996*, 80–88.

29. Pagel, J.M., Matthews, D.C., Appelbaum, F.R., Bernstein, I.D., and Press, O.W. (2002). The use of radioimmunoconjugates in stem cell transplantation. Bone Marrow Transplant. *29*, 807–816.

30. Burtner, C.R., Chandrasekaran, D., Santos, E.B., Beard, B.C., Adair, J.E., Hamlin, D.K., Wilbur, D.S., Sandmaier, B.M., and Kiem, H.P. (2015). (211)Astatine-Conjugated Monoclonal CD45 Antibody-Based Nonmyeloablative Conditioning for Stem Cell Gene Therapy. Hum. Gene Ther. *26*, 399–406.

31. Mamonkin, M., Rouce, R.H., Tashiro, H., and Brenner, M.K. (2015). A T-cell-directed chimeric antigen receptor for the selective treatment of T-cell malignancies. Blood *126*, 983–992.

32. Georgiadis, C., Rasaiyaah, J., Gkazi, S.A., Preece, R., Etuk, A., Christi, A., and Qasim, W. (2019). Universal' Fratricide-Resistant CAR T Cells Against T Cell Leukemia Generated By Coupled & Uncoupled Deamination Mediated Base Editing. Blood *134*, 3219.

33. Dai, Z., Mu, W., Zhao, Y., Jia, X., Liu, J., Wei, Q., Tan, T., and Zhou, J. (2021). The rational development of CD5-targeting biepitopic CARs with fully human heavy-chain-only antigen recognition domains. Mol. Ther. *29*, 2707–2722.

34. Gomes-Silva, D., Srinivasan, M., Sharma, S., Lee, C.M., Wagner, D.L., Davis, T.H., Rouce, R.H., Bao, G., Brenner, M.K., and Mamonkin, M. (2017). CD7-edited T cells expressing a CD7-specific CAR for the therapy of T-cell malignancies. Blood *130*, 285–296.

35. Dai, Z., Mu, W., Zhao, Y., Cheng, J., Lin, H., Ouyang, K., Jia, X., Liu, J., Wei, Q., Wang, M., et al. (2022). T cells expressing CD5/CD7 bispecific chimeric antigen receptors with fully human heavy-chain-only domains mitigate tumor antigen escape. Signal Transduct. Targeted Ther. *7*, 85.

36. Freiwan, A., Zoine, J.T., Crawford, J.C., Vaidya, A., Schattgen, S.A., Myers, J.A., Patil, S.L., Khanlari, M., Inaba, H., Klco, J.M., et al. (2022). Engineering naturally occurring CD7- T cells for the immunotherapy of hematological malignancies. Blood *140*, 2684–2696.

37. Velasquez, M.P., and Mamonkin, M. (2022). CD7 CAR: sword and shield. Blood *140*, 293–294.

38. Gomes-Silva, D., Atilla, E., Atilla, P.A., Mo, F., Tashiro, H., Srinivasan, M., Lulla, P., Rouce, R.H., Cabral, J.M.S., Ramos, C.A., et al. (2019). CD7 CAR T Cells for the Therapy of Acute Myeloid Leukemia. Mol. Ther. *27*, 272–280.

39. Glisovic-Aplenc, T., Diorio, C., Chukinas, J.A., Veliz, K., Shestova, O., Shen, F., Nunez-Cruz, S., Vincent, T.L., Miao, F., Milone, M.C., et al. (2023). CD38 as a pan-hematologic target for chimeric antigen receptor T cells. Blood Adv *7*, 4418–4430.

40. Gao, Z., Tong, C., Wang, Y., Chen, D., Wu, Z., and Han, W. (2019). Blocking CD38-driven fratricide among T cells enables effective antitumor activity by CD38-specific chimeric antigen receptor T cells. J Genet Genomics *46*, 367–377.

41. Lin, Y., Pagel, J.M., Axworthy, D., Pantelias, A., Hedin, N., and Press, O.W. (2006). A genetically engineered anti-CD45 single-chain antibody-streptavidin fusion protein for pretargeted radioimmunotherapy of hematologic malignancies. Cancer Res. *66*, 3884–3892.

42. Ruffner, K.L., Martin, P.J., Hussell, S., Nourigat, C., Fisher, D.R., Bernstein, I.D., and Matthews, D.C. (2001). Immunosuppressive effects of (131)I-anti-CD45 antibody in unsensitized and donor antigen-presensitized H2-matched, minor antigen-mismatched murine transplant models. Cancer Res. *61*, 5126–5131.

43. Watanabe, N., Mo, F., Zheng, R., Ma, R., Bray, V.C., van Leeuwen, D.G., Sritabal-Ramirez, J., Hu, H., Wang, S., Mehta, B., et al. (2023). Feasibility and preclinical efficacy of CD7-unedited CD7 CAR T cells for T cell malignancies. Mol. Ther. *31*, 24–34.

44. Laskowski, T.J., Biederstädt, A., and Rezvani, K. (2022). Natural killer cells in antitumour adoptive cell immunotherapy. Nat. Rev. Cancer *22*, 557–575.

45. Glienke, W., Esser, R., Priesner, C., Suerth, J.D., Schambach, A., Wels, W.S., Grez, M., Kloess, S., Arseniev, L., and Koehl, U. (2015). Advantages and applications of CAR-expressing natural killer cells. Front. Pharmacol. *6*, 21.

46. Ho, M.S.H., Medcalf, R.L., Livesey, S.A., and Traianedes, K. (2015). The dynamics of adult haematopoiesis in the bone and bone marrow environment. Br. J. Haematol. *170*, 472–486.

47. Chan, Y.Y., Ho, P.Y., Swartzrock, L., Rayburn, M., Nofal, R., Thongthip, S., Weinberg, K.I., and Czechowicz, A. (2023). Non-genotoxic Restoration of the Hematolymphoid System in Fanconi Anemia. Transplant. Cell. Ther. *29*, 164.e1–164.e9.

48. Li, Z., Czechowicz, A., Scheck, A., Rossi, D.J., and Murphy, P.M. (2019). Hematopoietic chimerism and donor-specific skin allograft tolerance after non-genotoxic CD117 antibody-drug-conjugate conditioning in MHC-mismatched allotransplantation. Nat. Commun. *10*, 616.

49. Gao, C., Schroeder, J.A., Xue, F., Jing, W., Cai, Y., Scheck, A., Subramaniam, S., Rao, S., Weiler, H., Czechowicz, A., and Shi, Q. (2019). Nongenotoxic antibody-drug conjugate conditioning enables safe and effective platelet gene therapy of hemophilia A mice. Blood Adv. *3*, 2700–2711.

50. Saha, A., and Blazar, B.R. (2022). Antibody based conditioning for allogeneic hematopoietic stem cell transplantation. Front. Immunol. *13*, 1031334.

51. Nakamae, H., Wilbur, D.S., Hamlin, D.K., Thakar, M.S., Santos, E.B., Fisher, D.R., Kenoyer, A.L., Pagel, J.M., Press, O.W., Storb, R., and Sandmaier, B.M. (2009). Biodistributions, myelosuppression, and toxicities in mice treated with an anti-CD45 antibody labeled with the alpha-emitting radionuclides bismuth-213 or astatine-211. Cancer Res. *69*, 2408–2415.

52. Friesen, C., Glatting, G., Koop, B., Schwarz, K., Morgenstern, A., Apostolidis, C., Debatin, K.M., and Reske, S.N. (2007). Breaking chemoresistance and radioresistance with [213Bi]anti-CD45 antibodies in leukemia cells. Cancer Res. *67*, 1950–1958.

53. Chen, Y., Kornblit, B., Hamlin, D.K., Sale, G.E., Santos, E.B., Wilbur, D.S., Storer, B.E., Storb, R., and Sandmaier, B.M. (2012). Durable donor engraftment after radioimmunotherapy using alpha-emitter astatine-211-labeled anti-CD45 antibody for conditioning in allogeneic hematopoietic cell transplantation. Blood *119*, 1130–1138.

54. Pagel, J.M., Gooley, T.A., Rajendran, J., Fisher, D.R., Wilson, W.A., Sandmaier, B.M., Matthews, D.C., Deeg, H.J., Gopal, A.K., Martin, P.J., et al. (2009). Allogeneic hematopoietic cell transplantation after conditioning with 131I-anti-CD45 antibody plus fludarabine and low-dose total body irradiation for elderly patients with advanced acute myeloid leukemia or high-risk myelodysplastic syndrome. Blood *114*, 5444–5453.

55. Vo, P., Gooley, T.A., Rajendran, J.G., Fisher, D.R., Orozco, J.J., Green, D.J., Gopal, A.K., Haaf, R., Nartea, M., Storb, R., et al. (2020). Yttrium-90-labeled anti-CD45 antibody followed by a reduced-intensity hematopoietic cell transplantation for patients with relapsed/refractory leukemia or myelodysplasia. Haematologica *105*, 1731–1737.

56. Tuazon, S.A., Cassaday, R.D., Gooley, T.A., Sandmaier, B.M., Holmberg, L.A., Smith, S.D., Maloney, D.G., Till, B.G., Martin, D.B., Chow, V.A., et al. (2021). Yttrium-90 Anti-CD45 Immunotherapy Followed by Autologous Hematopoietic Cell Transplantation for Relapsed or Refractory Lymphoma. Transplant. Cell. Ther. *27*, 57.e1–57.e8.

57. Srikanthan, M.A., Humbert, O., Haworth, K.G., Ironside, C., Rajawat, Y.S., Blazar, B.R., Palchaudhuri, R., Boitano, A.E., Cooke, M.P., Scadden, D.T., and Kiem, H.P. (2020). Effective Multi-lineage Engraftment in a Mouse Model of Fanconi Anemia Using Non-genotoxic Antibody-Based Conditioning. Mol. Ther. Methods Clin. Dev. *17*, 455–464.

58. Kung, C., Pingel, J.T., Heikinheimo, M., Klemola, T., Varkila, K., Yoo, L.I., Vuopala, K., Poyhonen, M., Uhari, M., Rogers, M., et al. (2000). Mutations in the tyrosine phosphatase CD45 gene in a child with severe combined immunodeficiency disease. Nat. Med. *6*, 343–345.

59. Wellhausen, N., O'Connell, R.P., Lesch, S., Engel, N.W., Rennels, A.K., Gonzales, D., Herbst, F., Young, R.M., Garcia, K.C., Weiner, D., et al. (2023). Epitope base editing CD45 in hematopoietic cells enables universal blood cancer immune therapy. Sci. Transl. Med. *15*, eadi1145.

60. Budde, L.E., Berger, C., Lin, Y., Wang, J., Lin, X., Frayo, S.E., Brouns, S.A., Spencer, D.M., Till, B.G., Jensen, M.C., et al. (2013). Combining a CD20 chimeric antigen receptor and an inducible caspase 9 suicide switch to improve the efficacy and safety of T cell adoptive immunotherapy for lymphoma. PLoS One *8*, e82742.

61. Kieback, E., Charo, J., Sommermeyer, D., Blankenstein, T., and Uckert, W. (2008). A safeguard eliminates T cell receptor gene-modified autoreactive T cells after adoptive transfer. Proc. Natl. Acad. Sci. USA *105*, 623–628.

62. Stepanov, A.V., Kalinin, R.S., Shipunova, V.O., Zhang, D., Xie, J., Rubtsov, Y.P., Ukrainskaya, V.M., Schulga, A., Konovalova, E.V., Volkov, D.V., et al. (2022). Switchable targeting of solid tumors by BsCAR T cells. Proc. Natl. Acad. Sci. USA *119*, e2210562119.

63. Stepanov, A.V., Xie, J., Zhu, Q., Shen, Z., Su, W., Kuai, L., Soll, R., Rader, C., Shaver, G., Douthit, L., et al. (2023). Control of the antitumour activity and specificity of CAR T cells via organic adapters covalently tethering the CAR to tumour cells. Nat. Biomed. Eng. *8*, 529–543.

64. Wang, X., Chang, W.C., Wong, C.W., Colcher, D., Sherman, M., Ostberg, J.R., Forman, S.J., Riddell, S.R., and Jensen, M.C. (2011). A transgene-encoded cell surface polypeptide for selection, in vivo tracking, and ablation of engineered cells. Blood *118*, 1255–1263.

65. Denman, C.J., Senyukov, V.V., Somanchi, S.S., Phatarpekar, P.V., Kopp, L.M., Johnson, J.L., Singh, H., Hurton, L., Maiti, S.N., Huls, M.H., et al. (2012). Membrane-bound IL-21 promotes sustained ex vivo proliferation of human natural killer cells. PLoS One *7*, e30264.

66. Ukrainskaya, V., Rubtsov, Y., Pershin, D., Podoplelova, N., Terekhov, S., Yaroshevich, I., Sokolova, A., Bagrov, D., Kulakovskaya, E., Shipunova, V., et al. (2021). Antigen-Specific Stimulation and Expansion of CAR-T Cells Using Membrane Vesicles as Target Cell Surrogates. Small *17*, e2102643.

67. Ukrainskaya, V.M., Musatova, O.E., Volkov, D.V., Osipova, D.S., Pershin, D.S., Moysenovich, A.M., Evtushenko, E.G., Kulakovskaya, E.A., Maksimov, E.G., Zhang, H., et al. (2023). CAR-tropic extracellular vesicles carry tumor-associated antigens and modulate CAR T cell functionality. Sci. Rep. *13*, 463.